4 Periglacial features around Tiksi

Guido Grosse, Lutz Schirrmeister, Viktor Kunitsky and Alexander Dereviagyn

4.1 Aims and study area

The study of the recent periglacial environment in combination with former periglacial processes helps to reconstruct the Quaternary landscape history of the Arctic coastal region. Of special interest are relationships between the areas of coastal lowlands and the adjoining coastal ranges. Consequently, the area around Tiksi is quite suitable for studying periglacial processes in both landscape types. The investigation area extends from the Khorogor Valley in the north to the Sevastyan Lake in the south and includes the Bykovsky Peninsula in the east (Figure 4-1). Our studies focused on five topics:

1. The observation, characterisation, geodetic survey and sampling of various periglacial surface phenomenons like ice wedge polygons, cryoplanation terraces, thermokarst structures, nival niches, snowfields, pingos and lagoons. The results serve as field verification of typical periglacial structures for the interpretation of remote sensing data. For that purpose the study objects were characterized qualitatively by collecting surface samples, measuring soil temperature and –moisture on a mobile soil probe and photographical documentation. Shape, extension and position were determined by laser tachymeter (Zeiss ELTA 3) or by measuring tape.

2. To determine the influence of modern nival processes on the Arctic landscape genesis recent snowfields and their surroundings were studied concerning size, structure and composition of snow and sediments. As is known, there is the assumption that a close connection exists between the Ice Complex genesis in the Laptev Sea coastal lowlands and the occurrence of perennial snowfields or embryonic glaciers within close mountain ranges during the Pleistocene (Galabala 1997, Kunitsky 1987). The new studies are connected with former work in the Chekanovsky Ridge and on Bol'shoy Lyakhovsky Island (Kunitsky et al. 2002).

3. Around Tiksi traces of glacial conditions were re-investigated (drumlin-, glacial boulder-and moraine-like features), which serve as evidence for an arctic shelf glacier according to Grosswald & Spektor (1993).

4. Investigation of exposed permafrost deposits (thermokarst mounds, coastal outcrops) as supplement to previous studies carried out on the Bykovsky Peninsula (Schirrmeister et al. 2002).

5. Investigation of recent processes of ground ice formation using stable isotope and tritium methods. The isotopic composition (^{3}H, $\delta^{18}O$, δD) of both types of ground ice (texture ice and ice wedges) and of various forms of water and (rain, snow, suprapermafrost groundwater, surface water) was studied.

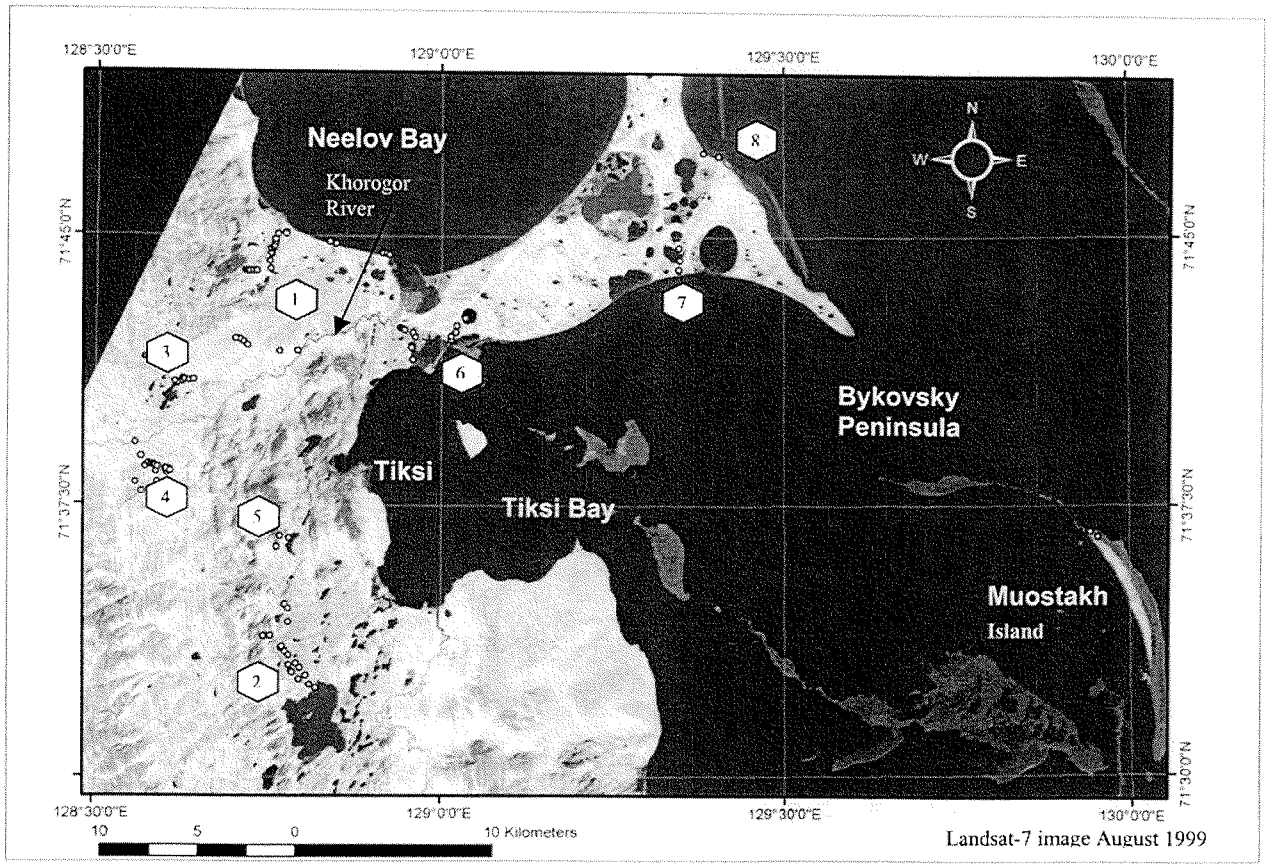

Figure 4-1: Overview map of the region around Tiksi: 1 – Khorogor Valley; 2 – Sevastyan Lake; 3 – Figurnoye Lake; 4 – upper Khorogor Valley with terraces; 5 – nival monitoring site; 6 – old Khorogor Delta; 7 – Polar Fox Lake; 8 – Mamontovy Khayata & Mamontovy Bulgunnyaga; small circles represent investigation sites

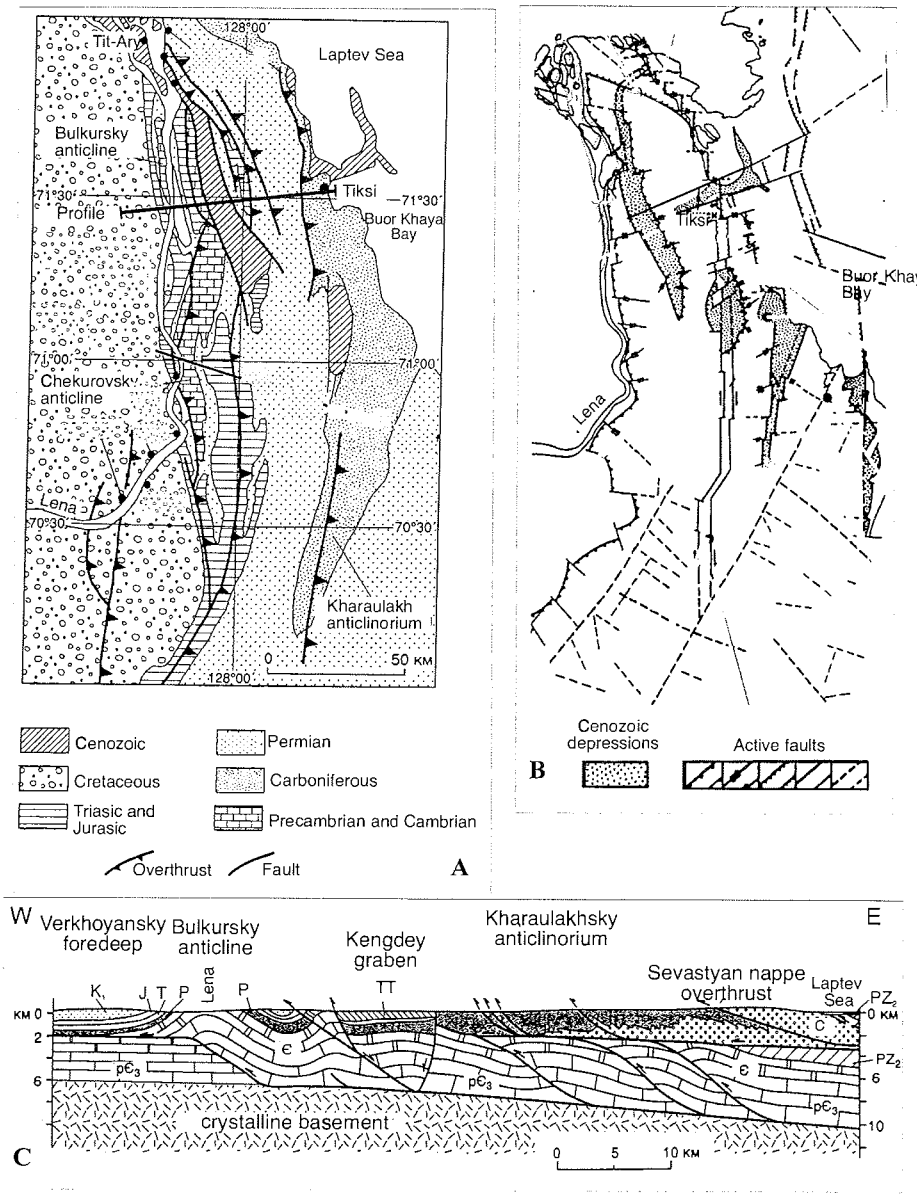

Figure 4-2: Schematic geological map (A) of the Kharaulakh region, tectonical map of modern active faults (B) and the E-W-profile across the Kharaulakh Ridge near Tiksi (C); according to Imaev et al. (2000) and Parfenov (2001).

The area in the region of Tiksi is subdivided into two main parts - the coastal mountain range of the Kharaulakh Ridge in the west and the remains of a former accumulation plain including the Bykovsky Peninsula in the east. The mountains close to Tiksi between the Khorogor Valley and Sevastyan Lake

belong to the Kharaulakhsky anticlinorium (Parfenov 2001). This area is situated within the central zone of the Kharaulakh seismotectonical zone (Imaev et al. 2000). The entire region of the Kharaulakh Ridge between the Lena River and the Laptev Sea is shaped by Cretaceous overthrust tectonics and Cenozoic block tectonics (Figure 4-2). The geological and tectonical evolution of the concerned area is controlled by position at the boundary between the Eurasian and the North American plates. The intensely folded and imbricated rocks consist of Permo-Carboniferous sequences of sandstone-slate-beddings, which were assigned to a shallow shelf facies (Imaev et al. 2000).

During the pre-Cretaceous period the Siberian Plate had a passive margin in this region, where several kilometres of sediments of a Precambrian Mesozoic mega-complex had been accumulated. The lower Cretaceous main folding of the Verkhoyansky collision orogen resulted in typical compression tectonics. The Kharaulakhsky anticlinorium has to be interpreted as a blind autochthonous roof duplex structure with a subjacent overthrust plain to the crystalline basement and a roof overthrust plain, covered by upper Palaeozoic and early Mesozoic series (Figure 4-2). Overthrusts were generally orientated to the west, which is evident in asymmetrical to overturned folds. They are up to some hundred metres large with a western vergency. A special area is the Sevastyan nappe overthrust. The rocks there consist only of Carboniferous to lower Permian distal turbidites and contourites. They were overthrusted at the Kharaulakhsky seismo-tectonical zone. The associated foliation is inclined N to NNW.

The later geological and tectonical evolution is connected with the rift-genesis of the Gakkel Ridge and its extension on the continental plate (Ust Lena rift, Moma 'rift') (Drachev et al. 1998, Franke et al. 2000). Deposits of the Cenozoic mega-complex are mainly connected with the Tertiary graben system and cover the Precambrian-Mesozoic mega-complex with a strong discordance. The lignite deposits within the Sogo graben south of Tiksi belong to this complex, too. In addition, local compression during the Cenozoic period is evident by folding and overthrusting of Tertiary deposits. Tectonical uplift connected with peneplain formation in different heights within the Kharaulakh Ridge as well as block tectonics in the Lena delta and eastern Laptev Sea region were typical processes during Cenozoic times (Imaev et al. 2000). This is proved by dislocations of the Neogene weathering crust along the Buor Khaya Gulf coasts as well as by different base levels of the late Pleistocene to Holocene deposits within the Lena delta (Galabala 1980, Grigoriev 1993).

The relief in the central part of Kharaulakh Ridge is characterized by strong dissection. According to Imaev et al. (2000) deep-cutting, steep river valleys, ridge-like watersheds with peaks above, kars, small glaciers and numerous snowfields form an alpine character in this area. Flat upland areas of erosive-tectonical denudation origin were formed at the western and eastern slopes. The steps of these old peneplains are directly related to Cenozoic uplift. In addition, traces of mountain glacier activities like moraine deposits, trough shoulders and down-washed bottoms of old glacier valleys were reported by

Imaev et al. (2000) in various river valleys. There seem to be connections between the length of valleys and their orientations within the uplifting areas. Long valleys of some ten kilometres length are orientated to NE within dislocation zones. However, the N-S orientated valleys are clearly shorter (some km) and were formed by erosion of rocks like slate. The large u-shaped valleys connected with fracture zones have a broad, flat valley bottom, which is covered by patchwork-like tundra. Accumulation and pediment terraces of 2 to 15 m height above the valley bottom are typical at the slope base. The Kharaulakh Ridge are restricted to the east by an accumulation plain with a small inclination to the sea. Ice Complex hills, thermokarst depressions and valleys, thermokarst mounds and pingos are very common in this area.

According to Imaev et al. (2000) the Cenozoic landscape history of the Kharaulakh Ridge include an initial stage with uplift in the south during Eocene to early Oligocene and a major stage (late Oligocene to early Pleistocene), when the relief forming linear uplifts occurred. Only in the north an erosional denudation plain had already existed. During the final stage (middle Pleistocene to Holocene) a new uplift occurred which formed the present-day ridges and depressions and the related hydrological situation. Nowadays, tectonical movements still keep on, as is proven by seismic studies and levelling measurements. The oldest documented earthquake with a magnitude of 6.8 occurred near the Lena delta in 1909. Numerous earthquakes were recorded during the following years too, sometimes with magnitudes between 4 and 5.8. Therefore, the Quaternary landscape history of our study area is closely connected with neotectonic processes.

4.2. Periglacial phenomena of the eastern Khorogor valley

4.2.1. Between the rivers Vassily and Khorogor

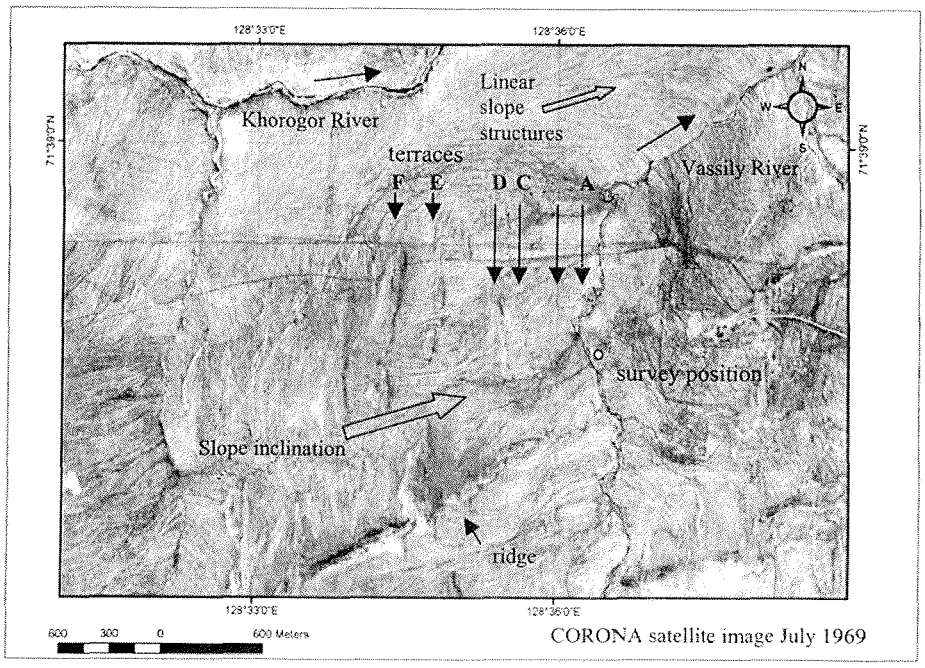

Figure 4-3: Overview map of the investigation area between the Vassily River and Khorogor river

In the area between the Vassily River and the Khorogor River a geodetic survey of cryoplanation terraces at valley slopes had been carried out within two days (Figure 4-3). On the first day the terrain was examined. A favourable location for the laser tachymeter was found and the boundaries of 6 terraces were marked with wooden sticks. On the second day we surveyed the terraces, named A to F, using some 157 measuring points which were situated on the upper and the lower edge of each terrace (Figure 4-4). For time reasons no points were measured between the terraces. Therefore, the density of points allows only a simple modelling of the terraces themselves, but not of the interspaces (Figure 4-4). A schematic slope profile shows that the terraces have their origin in the changing lithology and resistance of the sandstone-slate alternation in the basement (Figure 4-5). The terraces are more or less strictly N-S oriented whereas the slope is inclining to the east. The relief got its character with gently slopes by periglacial weathering and transport processes where the basement consists of soft slates and of flat terraces where the harder, more resistant sandstone layers occur. Only in a few places the bedrocks crop out. Mostly they are covered by weathering detritus and silty to sandy nivation deposits.

Table 4-1: Properties of the studied cryoplanation terraces area north of the Vassily River

Area	Height	Description	Sample
Terrace F	116 m	Several steep basset edges, coarse-grained debris, vegetation-debris-strips (2-3 m wide)	Khg-19-1
Area F-E	108 m	Vegetation cover 100 %, *Betula nana*, moss, slope inclination <5°, active layer depth 40-50 cm, loamy sand with small gravels, frost boils 30-80 cm, polygons 7-10 m	Khg-19-2
Terrace E		Vegetation cover 80%, mostly moss, coarse-grained debris	
Area E-D	90 m	Dense grass-moss-vegetation, meandering grass brooks (1.5 to 6 m wide), subsurface ice layer, moss peat patches (Ø 10 m) with frost cracks and ice wedge polygons, silty fine sand	Khg-95-12 Khg-19-3
Terrace D	84 m	Coarse-grained rock debris (Ø 10 to 20 cm), partly covers of mixtures of plant detritus and fine sand (Chionoconite)	Khg-19-6 Khg-19-5
Area D-C	82 m	Grass cover 100%, silty fine sand, only few gravels, frost boils, polygons, grass brook (2 m wide) with flat thermokarst mounds	Khg-19-7

The terraces are covered with stones (up to 15 cm in ∅) in a fine-grained matrix (Table 4-1). The processes occurring at these slopes are frost scattering of the basement at outcrops, solifluction and cryoturbation on the slopes and in the active layer, melt water runoff in spring, aeolian transport on the slope surfaces and at last accumulation of sediment material by the Vassily and Khorogor rivers. On the grass and moss covered plain between terraces E and D a transparent, 2-3cm thick ice layer with vertical ice needles was observed and sampled (Khg-95-12).

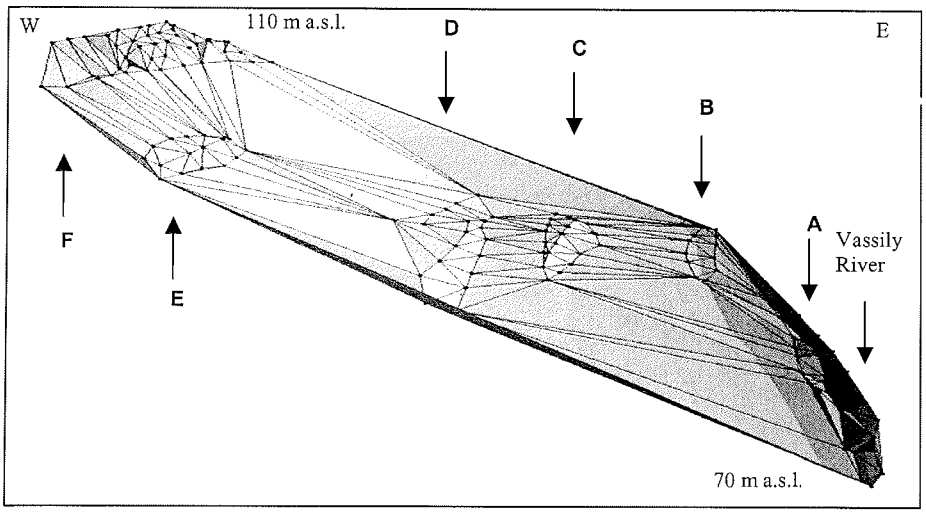

Figure 4-4: The height exaggerated 3-D model of the cryoplanation terrace survey

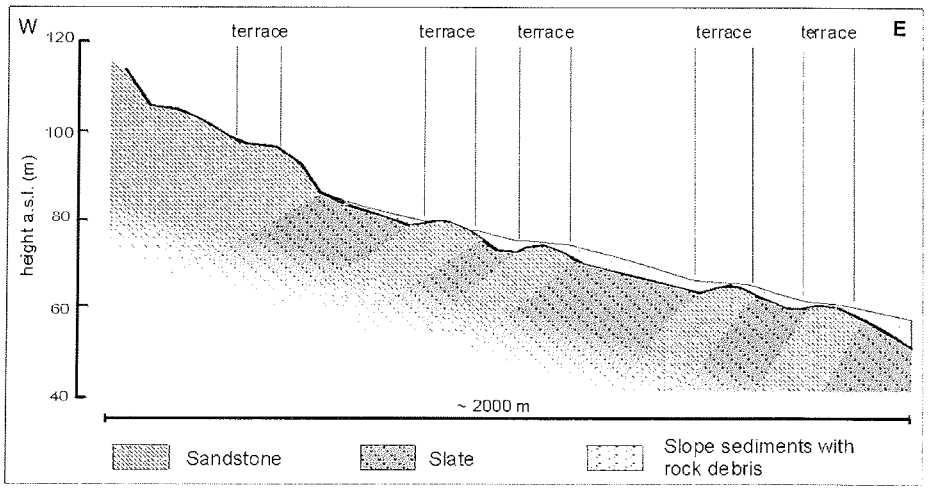

Figure 4-5: Schematic view for the lithological situation below the cryoplanation terraces

South of the cryoplanation terraces the basement crops out partially. In remote sensing images a ridge is clearly visible (Figure 4-3) cross-cutting the terraces from NE to SW. Its highest point is about 190 m a.s.l., so that the whole ridge overlooks the surrounding surface with relatively steep slopes. Beds of Permian sandstones and slates dominate the geology of the basement of this area with the same north-south striking direction like the terraces. Further, there are some dolerite dykes, which intruded into the sedimentary rocks (Figure 4-6). The differing hardness of these rocks is visible again by the shape of the geomorphological relief. The sandstones with calcareous cement and quartz filled fissures and the dolerites formed elevations and single rocks while the strongly weathered slates formed the depressions in the ridge. The ridge itself is covered only by coarse-grained weathering material but not by fine-grained sediments (Figure 4-7). Hence it is considered as one source area for sediment material on the terraces. The ridge could be an example for similar basement characteristics below the cryoplanation terraces. Several samples had been taken from outcropping rocks (Khg-2, Khg-3, Khg-4-1 & -2).

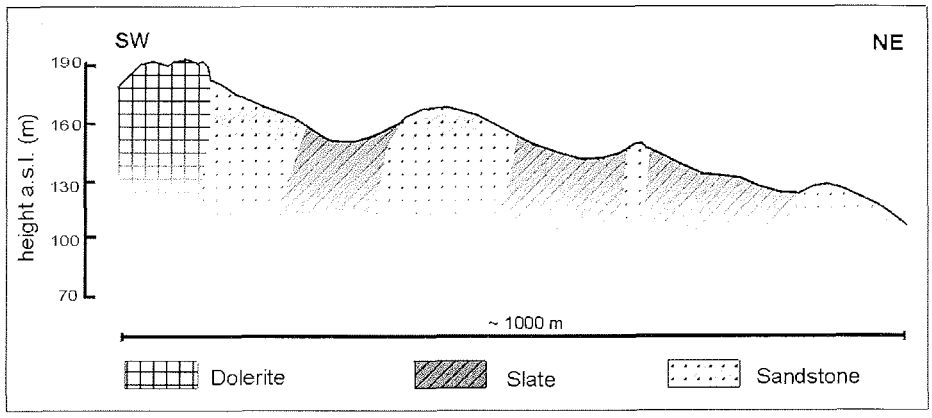

Figure 4-6: Geological situation of the ridge south of the cryoplanation terraces

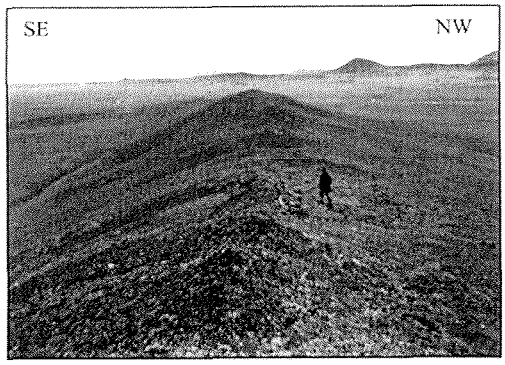

Figure 4-7: The bedrock ridge is covered only by coarse-grained frost weathering material

North of the cryoplanation terraces the Khorogor river is situated. Between terraces and the Khorogor River a gently inclined accumulation plain of about 1 km width has been formed. In this area silty to sandy sediments occur. Frost boils in that area contain only a few (near the river, sample Khg-5-1) or no pebbles at all (more south from the river, sample Khg-6).

The southern riverbank of the Khorogor River is a steep cliff of the same outcropping basement rocks as described above. The interbedding of sandstone and slates has a very steep inclination and seems to be folded in a large scale (Figure 4-8). The cliff is 6-8 m high and the discordant sedimentary layer on top is approximately 1 m thick. The river water was sampled there (Khg-96-1) as well as the black coarse-grained river sand.

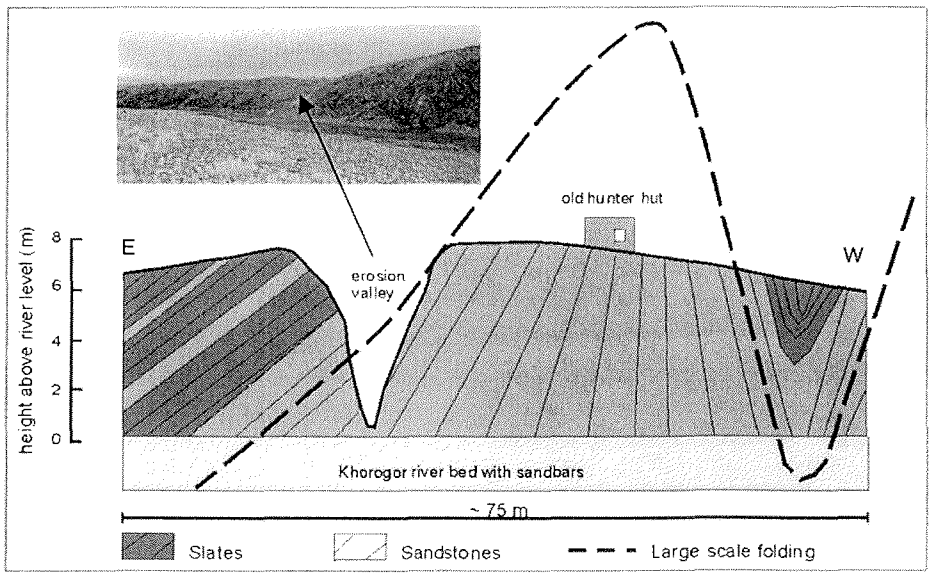

Figure 4-8: Bank of the Khorogor River with steep inclined sandstone-slate interbedding and large scale folding.

On the lowermost river terrace of the Vassily River several frost boils were found. The terrace was gently inclined towards the river and the vegetation on the terrace was dominated by moss, grass and species of Salix and Betula. The diameters of the frost boils varied between 40 and 100 cm. One frost boil was excavated and described in detail (Figure 4-9). A cross section of active layer depths (Figure 4-10) around the frost boil showed, that the largest depth with 43 cm was found at the centre of the frost boil. With greater distance from the frost boil the active layer depth decreased to 20-25 cm.

Figure 4-9: Frost boil at the Vassily River terrace

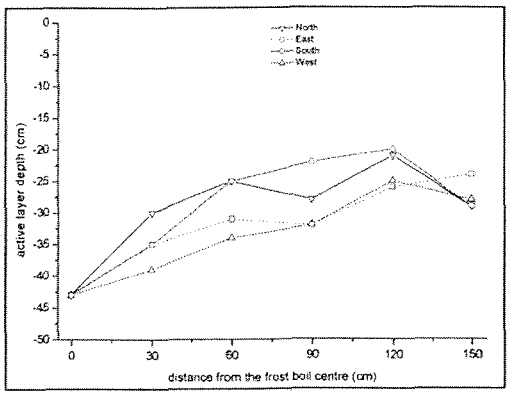

Figure 4-10: Active layer depth on 1st of August around the investigated frost boil

The surface of the frost boil consisted of dry, silty to fine grained sandy material (Figure. 4-11). Some small gravels (1 cm in ∅) were found in the centre of the surface. The upper horizon of loamy silty fine sand is about 30 cm deep and has a very low water content. Only a few grass roots were found, showing that the frost boil is still active. This upper part is irregularly interstratified by oxidative (brown) and reductive (grey-black) spots. The material is not laminated in a certain way. Below this horizon a thin water-saturated layer with a higher clay content and a reduced milieu is situated. Within the clayish matrix many pebbles were found (2-8 cm in ∅). At about 45 cm depth the ice containing permafrost starts with fine- to medium grained sand rich in pebbles. From the frost boil two samples were taken, one from the upper dry horizon (Khg-20-2) and one from the lower wet and reduced horizon (Khg-20-1).

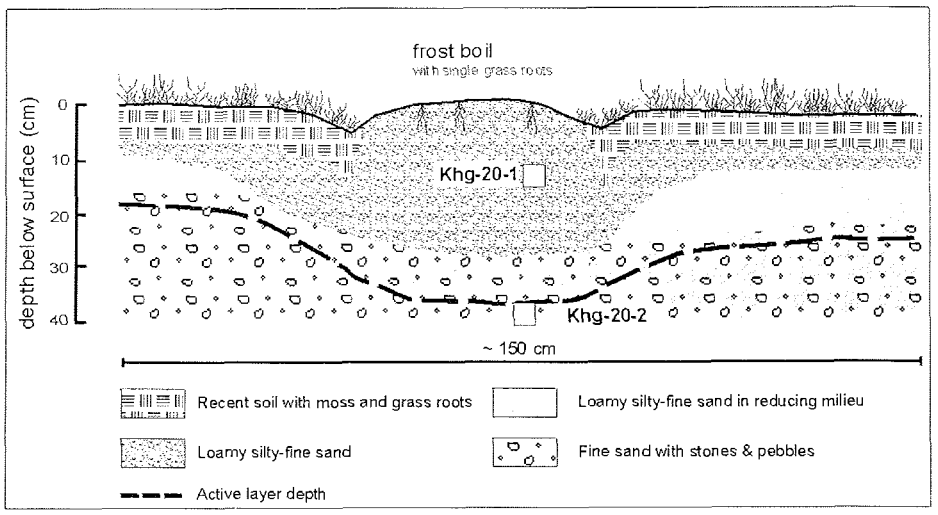

Figure 4-11: Schematic section across a frost boil at the Vassily River terrace

Approximately 1 km N of our terrace survey position we investigated a landscape on a gently inclined slope within a wet grass tundra setting. In the CORONA satellite image runoff structures, so-called "delly", were observed in that area (Figure 4-3, upper right corner). These structures were visible in the image as elongated parallel stripes oriented into the direction of the slope inclination, producing a fan-like widening with decreasing relief energy. These structures usually end at larger discharges like the Vassily River. Although we believed to find easily its expression in vegetation or relief differences on the ground, in the field we could not observe these structures. One assumption is, that they are more or less discharging in the active layer (subsurface), another assumption is, that episodic precipitation events cause these strips (surface). On explanation for dellies as initial thermokarst features on hill slopes is given by Katasonova (1963).

On the same slope, in a position equal to the lowest cryoplanation terrace, some polygons were found. A profile for active layer depths was measured (Figure 4-12) and a sediment sample (Khg-7) and an ice sample (Khg-95-1) was taken from a young ice wedge of about 15 cm wide below a frost crack. Here, too, frost boils occurred with diameter of 60-90 cm and active layer depths down to 40 cm.

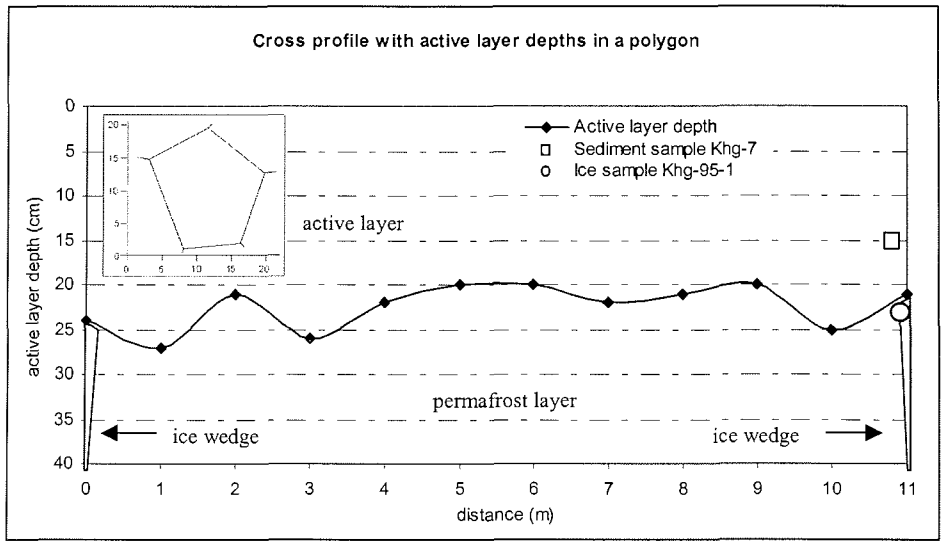

Figure 4-12: Active layer profile (1st August), size of the polygon and sample position for Khg-7 and Khg-95-1

On the northern upper slope of the Vassily River groundwater and an ice wedge were sampled near some buildings in a small pit (Khg-98-3, Khg-95-9). More ice, ground and surface water were sampled about 200 m lower at the slope within an ice wedge polygon (Khg-95-10 & 11, Khg-98-4, Khg-96-9 & 10).

4. 2. 2. Between Khorogor River and Lake Figurnoe

The area between the Khorogor River and Lake Figurnoe east of the settlement Tiksi 3 represents the plane, 2 to 3 km wide central part of the lower Khorogor Valley. Large ice wedge polygons and thermokarst mounds at the less inclined southern valley slopes possibly reflect the existence of a thin horizon of Ice Complex-like deposits there. The valley bottom has heights between 40 and 50 m a.s.l., and it is covered by a wet grass-tundra. Numerous peat patches (up to 40 m x 20 m) and peat circles (15 to 20 m in Ø) occur in distances between 30 to 50 m. These may represent former peat filled small ponds. Polygonal nets of different generations were observed within such peat patches. Large polygons (about 9 m in Ø) are subdivided into smaller polygons with diameters between 1 and 2 m.

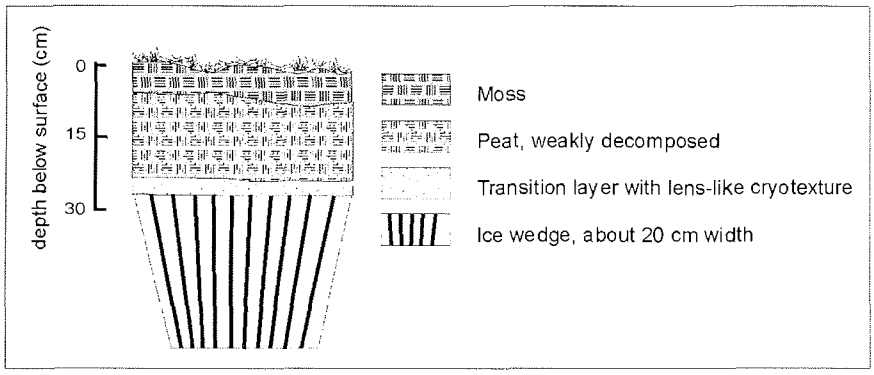

Figure 4-13: Pit Khg-8 with peat layers above an ice wedge

Additionally, frost boils are irregularly distributed in the whole area. In parts gravels and weakly subrounded stones (size 7-15 cm) of sandstone are concentrated in the centres of the frost boils. Therefore, the debris layer of the Khorogor valley should not be very deep below the surface. Other frost boils contain only silty fine sand. The active layer thickness varied between 40-60 cm in frost boils, 20 cm above frost cracks and between about 30-40 cm in polygonal sites. The material from the frost boils is transported by cryoturbation from greater depths up to 40-60 cm and might be useful as indicator for the basement below. Therefore the differences in the gravel content are most likely caused by the changing relief structure of the basement, which is composed by tilted alternations of more resistant sandstone and less resistant slate layers (Figure 4-14).

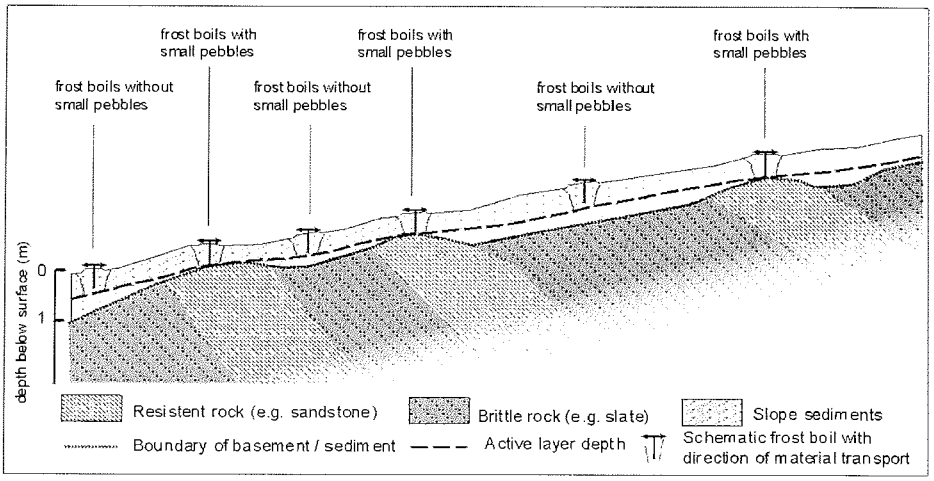

Figure 4-14: Schematic view of the occurrence of frost boils with material content of different grain sizes

All frost boils, which were investigated in more detail in the region around Tiksi are listed in table 4-2.

Table 4-2: Investigated frost boils in the region around Tiksi with their most characteristic properties (1st week of August)

Frost boil	Location and geomorphological position	Size (∅)	Lithology	Active layer depth	
				Frost boil	Surrounding
Khg-1	Flat plain at the base of the cryoplanation terraces; grass tundra	60 cm	Silty fine sand with pebbles (8 cm)	40 cm	35-40 cm
	Upper terraces, flat plain; sparse vegetation	200 cm	Fine sand with pebbles	45-50 cm	30-35 cm
Khg-5-1	Gently inclined plain towards the Khorogor River; grass tundra	35 cm	Silty fine sand with pebbles (6 cm)	45 cm	35-40 cm
Khg-6	Base of a moderate inclined slope towards the Khorogor River; dense, wet grass tundra	70 cm	Silty fine sand	52 cm	35 cm
	Former winter airport landing site; wet grass-moss tundra		Silty fine sand	50-57 cm	30-40 cm
Khg-9	Former winter airport landing site, within a large moss patch (15 x 30 m); wet grass-moss tundra	150 cm	Silty sand with quartz gravels	55 cm	
Khg-15	Flat plain in the northern part of the central Khorogor Valley, covered densely by frost boils; moss-lichen tundra	60 cm	Silty fine sand with gravels	50 cm	25 cm
Khg-19-2	Gently inclined slope between the cryoplanation terraces; dry grass tundra with mosses and Betula		Silty sand with unrounded pebbles	40-50 cm	
Khg-19-3	Gently inclined slope between the cryoplanation terraces; dry grass tundra	60-70 cm	Clayey fine sand with a few little rounded pebbles	40-50 cm	
Khg-19-7	Gently inclined slope between the cryoplanation terraces; dry grass tundra	60 cm	Silty fine sand		
Khg-20	Bank of the Vassily River, gently inclined slope; grass-moss tundra	50 cm	Loamy-silty fine sand	43 cm	20-35 cm
	Shore of the Neelov Bay near the recent Khorogor Delta, flat plain; wet grass tundra	180-200 cm	Silty sand with gravels	58 cm	25-43 cm
	Western Bykovsky Peninsula, evolving thermo-erosion valley; moss-lichen tundra		Silty fine sand		17-30 cm

The active layer close to a modern ice wedge was studied in detail and sampled in a small pit (Figure 4-13). It consisted of a 2 cm thick transition layer with lens-like cryostructure, a 20 cm thick layer of brownish weakly decomposed unfrozen peat and a 5 cm thick moss cover (Khg-8-1 to 8-3). Crossing the valley several samples were taken from a modern ice wedge (Khg-95-2), from ground water within our working pits (Khg-98-1, 2) and from surface water of the Khorogor River (Khg-96-3) and a small pond (Khg-96-4).

The surface of the valley bottom rises up to 80 m a.s.l. in the west and there the flat grass plain is delimited by Lake Figurnoe. In contrast to the circular shallow thermokarst ponds often observed this large lake has an irregular shape and seems to be much deeper. Weathered rocks of interbedding slates and fine-grained quartzitic sandstone surround the lake (Figure 4-15). Therefore it is assumed that Lake Figurnoe is of tectonic origin. The gently inclined slope towards the lake of about 200 to 300 m width is covered by weakly subrounded alluvial debris with sandstone pebbles of up to 10 cm and slate gravels of 1 to 2 cm size (Khg-10-4 and 5). Similar debris was observed within frost boils as described above. However, angular sandstone and slate debris were observed on the lake bottom near the shore. Again the lake water (Khg-96-5) and the lake bottom deposits (Khg-10-3) were sampled.

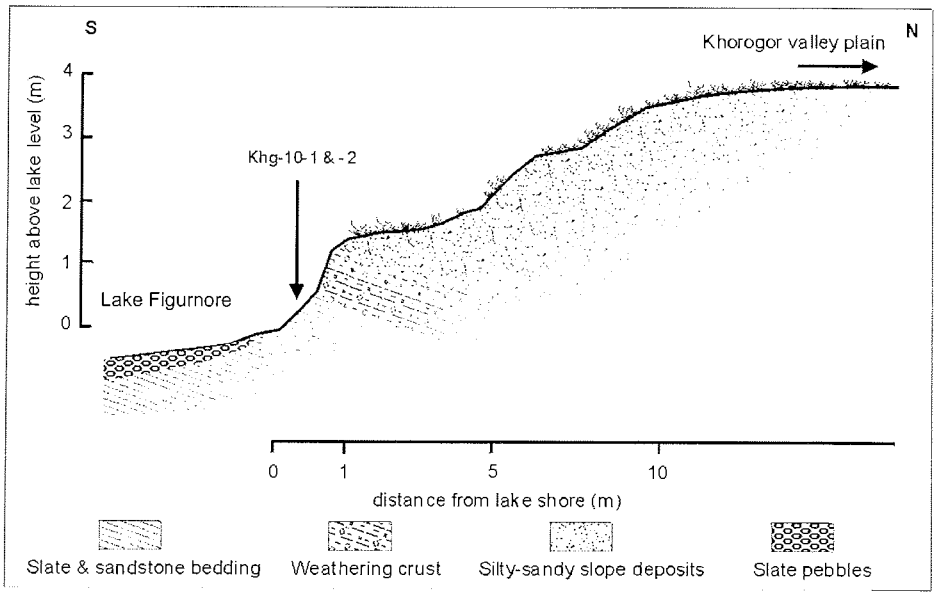

Figure 4-15: Cross profile of Lake Figurnoe northern slope

The area covered by dense grass tundra is bounded in the south by debris slopes with small inclination towards the Khorogor River (Figure 4-16A). On these slopes some larger boulders (50 – 70 cm in Ø) with weakly rounded edges and a bent and angular shaped surface structures were found (Figure 4-16B). This might be the area of a so-called boulder fan of a washed-out glacial moraine deposit (Grosswald & Spektor 1993). According to our interpretation the coarse grained debris is of fluvial or alluvial origin.

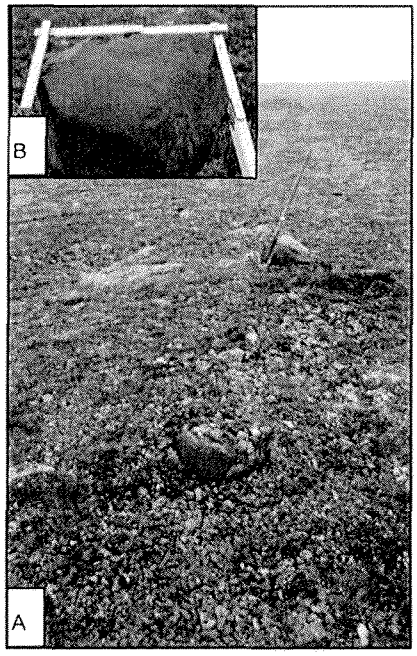

Figure 4-16: Debris slopes with large partially rounded boulders near Lake Figurnoe

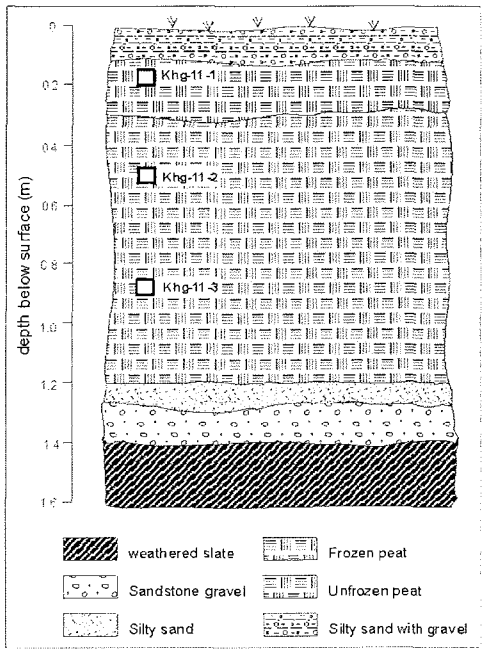

Figure 4-17: Profile Khg-11 of a thermokarst mound on the way near the Khorogor River

Thermokarst mounds were studied in the area further east of Lake Figurnoe on the way to the Khorogor River. They indicate thicker permafrost deposits and the occurrence of thermokarst processes. Our profile covers the permafrost horizon down to the weathering crust of the basement (Figure 4-17). The profile is composed of slate debris, a thin layer of pebbles, a thin layer of organic-rich, an about 1 m thick horizon of weakly decomposed moss peat (Khg-11-1 to 3) and a cover of a 0.5 m thick mixture of fine grained silty sand and gravels. This sequence reflects a development starting with fluvial processes, followed by accumulation within stagnant water of an old river branch, which was silted-up with moss peat and buried by a solifluction cover or by alluvial deposits.

4.2.3. Between the rivers Khorogor and Khatys-Yuryakh – the mouth of the Khorogor valley

The Khorogor Valley opens to the Neelov Bay in the area northwest of Tiksi airport. The valley here is bounded by the rivers Khorogor in the southeast and the Khatys-Yuryakh in the northwest and it has a width of about 7 km (Figure 4-18). The area is like a plain with a very gentle inclination towards the Neelov Bay and both rivers. In high-resolution satellite images a wide net of surface water dischargers is visible which are best explained with a delly-like development (Katasonova 1963). Many lakes occur there in the shore area of the Neelov Bay. A sharp boundary between the area of the lakes and the valley hinterland without lakes can be observed 1.5-2.0 km from the recent shoreline. Some of the lakes are supposed to be thermokarst lakes already, some are initial thermokarst lakes fed by surface runoff from the valley hinterland. Others contain coarse-grained fluvial material pointing to their origin in former fluvial beds. Meandering chains of small lakes indicate old river branches. In the north of the plain several initial flat thermo-erosional channels with depths of about one meter were observed. Their flow direction was towards the Khatys-Yuryakh River and the Neelov Bay. Anyway, the presence of thermokarst features in that region points to thicker ice-rich deposits in the ground than in the main part of the valley.

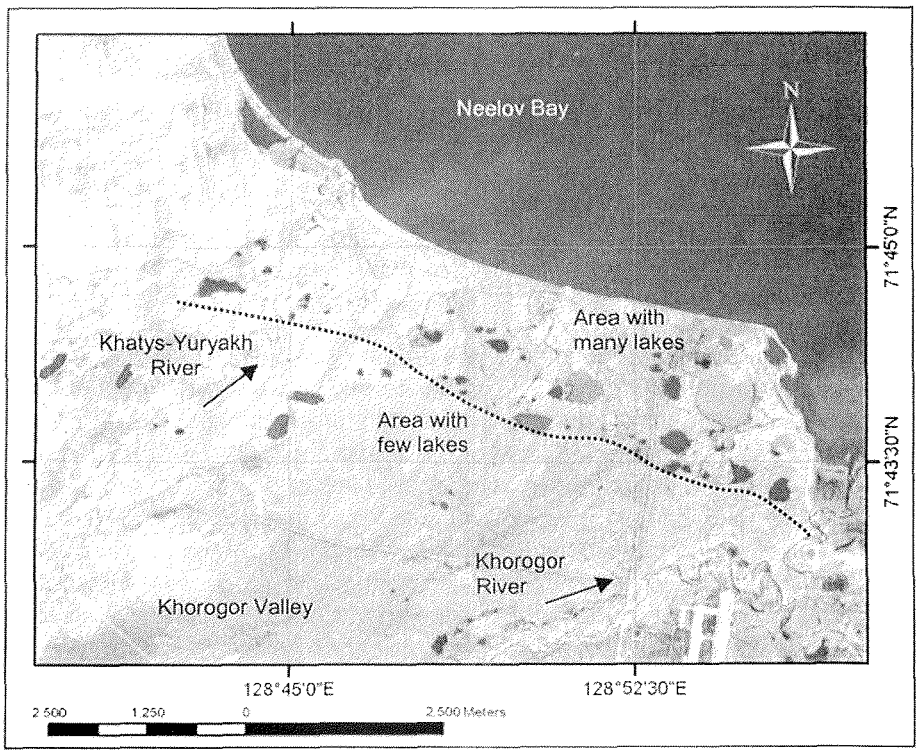

Figure 4-18: CORONA-Satellite image from July 1969 with the northeastern Khorogor Valley and the Neelov Bay shore

The central valley is dominated by typical moss-lichen (and few grass) tundra with polygonal patterns. The polygons had diameters from 8-20 m, and sometimes larger ones were split by younger frost crack generations. In several places dense moss patches with up to 25 m in diameter were found, possibly representing dried out shallow lakes. In other places standing water of 5-10 cm depth was found with grass vegetation. In places the polygons are still active as we found recent ice veins in polygonal frost cracks intruding older ice wedges. The recent ice vein had a width of only 1-3 cm while the older one had a width of about 18 cm. We sampled a recent ice vein (Khg-95-4), older ice wedges (Khg-95-3 and 5) and the surrounding sediment and soil (Khg-13-1 to 13-3) in two pits (Figure 4-19). The active layer depth in these polygons was between 15-35 cm.

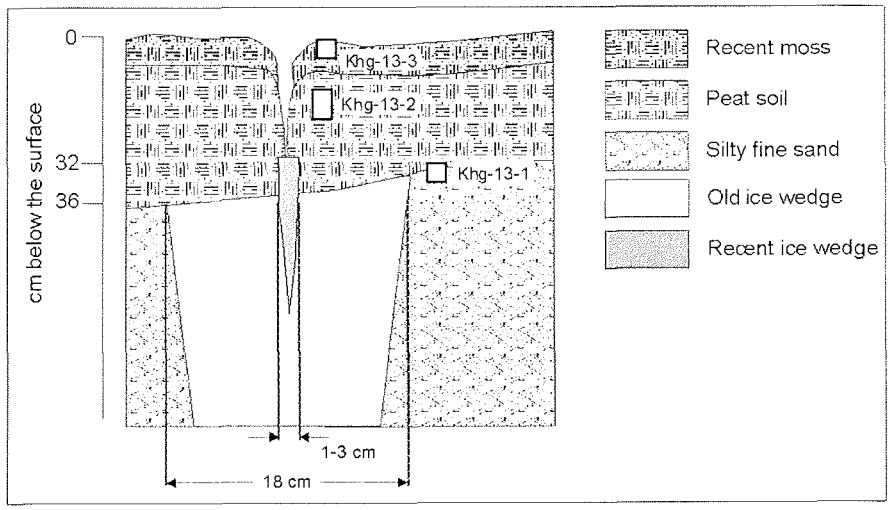

Figure 4-19: Pit Khg-13 with a recent ice vein intruding an older ice wedge

Other interesting features found in that area are frost mounds of which several were found in the central valley. Their conic shape is similar to known pingos but their size is much smaller with maximum one meter in height. The development is exemplarily interpreted for one investigated frost mound in Figure 4-20. They contain an ice lens, that is growing by subsurface water transport. Because the sediment layer on the basement is not very thick, as coarse-grained pebbles of the basement in the sediment indicate, the frost mound growth seems to be restricted to a certain height. The water comes from nearby water-filled polygonal troughs and has favourable transport conditions in the mixed grained sediment. The active layer thickness is decreased above the frost mound due to surface bulging. The thickness of the ice-lens could not be determined.

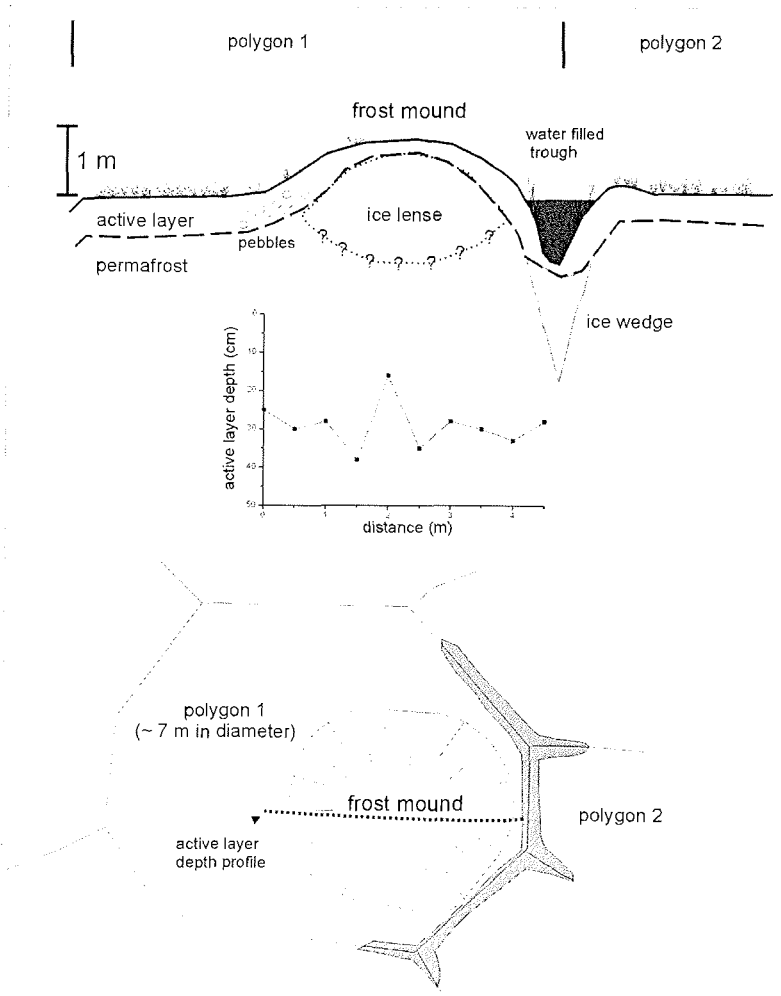

Figure 4-20: Frost mound in the central Khorogor Valley

Near the Khorogor River one of the lakes mentioned above was investigated in detail (Figure 4-21). It was more or less circular and had a diameter of about 40 m. The water and active layer depth was measured. The maximum water depth was 70 cm and the maximum active layer depth beneath the lake bottom was 45 cm. The rims of the lake were relatively steep. No talik was found below this shallow lake. This seems to be an initial stage of thermokarst. In another larger lake the coarse-grained bottom sediment was sampled (Khg-14-2). This lake might be a remnant of an old river branch.

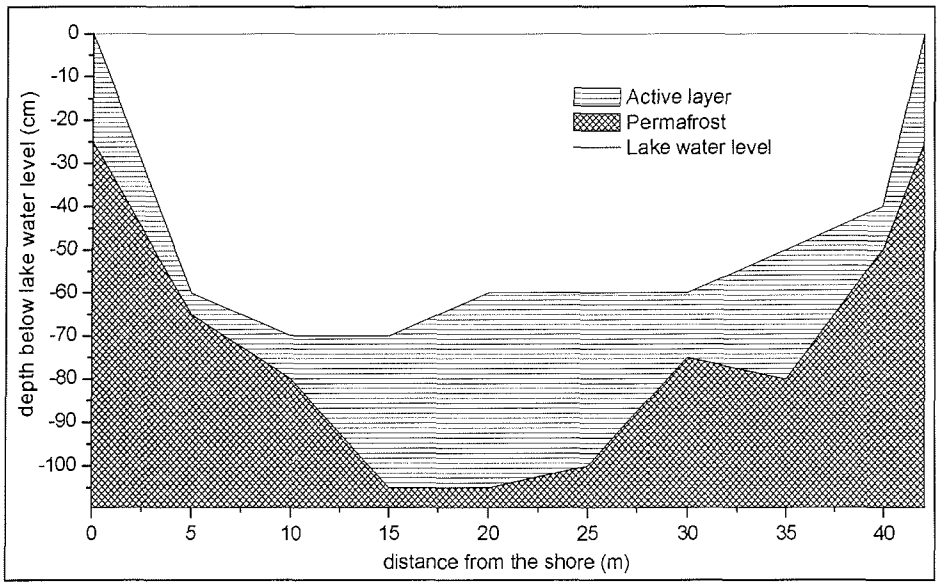

Figure 4-21: Lake profile with water depths and active layer depths (3rd August)

At the banks of the mouth of the Khorogor River several thermokarst mounds had formed, which point to ice-rich deposits, too. They were covered by a thick layer of unfrozen moss-peat and consisted mainly of frozen silty to sandy organic rich sediments. No regular ice texture was visible but ice intruded into root channels forming subvertical ice veins. One thermokarst mound was investigated in detail (Figure 4-22). The height of the riverbank in this locality was about 3 m. The riverbed itself was filled with medium- to coarse-grained sand and gravel. Several sediment samples were taken (Khg-17-1 to 12 from the thermokarst hill, Khg-16-1 and 2 from the river sediment).

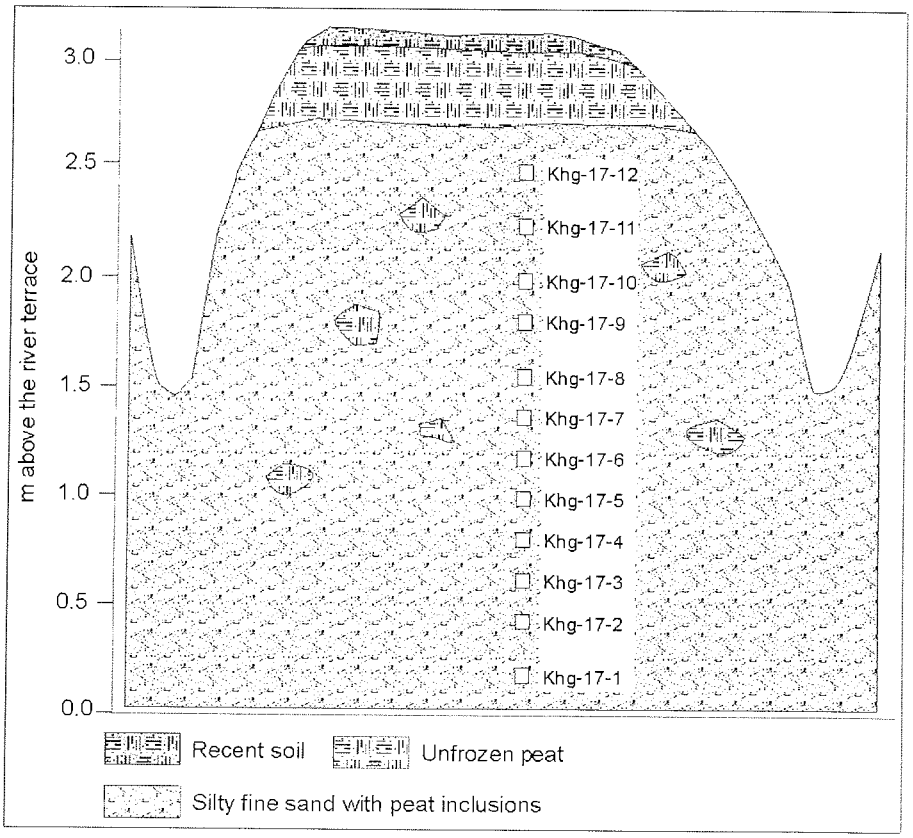

Figure 4-22: Thermokarst mound near the Khorogor river mouth with sediment sample positions

4.2.4. The old Khorogor River delta

The Khorogor River, running from the Kharaulakh Mountains towards the Bykovsky Peninsula is actually discharging into the Neelov Bay to the NE. An almost inactive old Khorogor delta has its mouth reaching to the SE into the Tiksi Bay (Figure 4-23). In this old delta only a few channels have a connection to the sea whereas many channels were separated and have become an elongated chain of lakes. Moss peat patches (Ø 15 m) occur with polygons of 0.3 m height and 1.5 m wide walls. The absolute height of the whole area is not more than 1-2 m a.s.l.. Thus, parts of the terraces are flooded through tidal or wind forced sea level high-stands, which is marked by driftwood trunks in the hinterland of the old delta. The area of the old delta is situated about 5 to 10 m deeper than the surroundings.

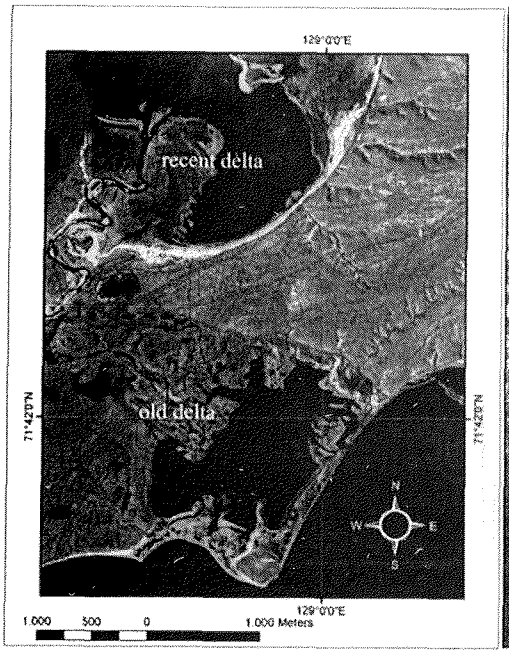

Figure 4-23: CORONA satellite map of the western Bykovsky Peninsula with the old and the recent Khorogor delta

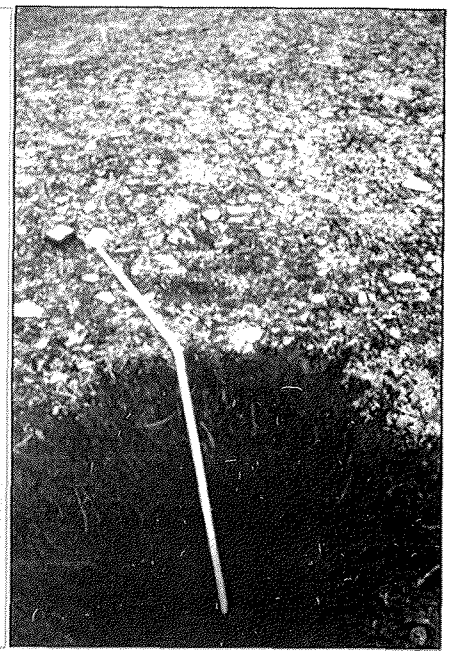

Figure 4-24: Sample pit for Khg-18-1 and Khg-18-2; note the pebble covered sediment surface

In general, the sediments have a matrix of middle-coarse grained light to dark grey sands with a high content of weakly rounded pebbles and stones. Within this river setting, which is thought to be similar to the early development stages of the basal layers of the Bykovsky Peninsula (Slagoda 1993), we observed the general sedimentological and geomorphological features. Further we investigated in detail some polygonal frost cracks of huge diameters on a gently inclined channel shore. In this place several generations of frost cracks were recognisable. We only surveyed the generation with the widest cracks, which also seemed to be the oldest, as other generations sometimes were only poorly

developed and had dead end cracks branching off with different angles from the wide cracks. The polygons have a more or less plain morphology while the crack itself is slightly lowered (5-10 cm) compared to the polygon centre. The polygonal structures are only poorly covered with vegetation, just the lowered cracks are covered more densely with grass and moss. In addition we took sediment samples (Khg-18-1 and Khg-18-2) from a pit in different depths down to 70 cm from a polygon centre (Figure 4-24). Active layer depths in the area varied from 30 to 100 cm.

For surveying we marked the junction points of the frost cracks with wooden sticks. The survey of 10 of the very irregular polygons on a very smooth slope (less than 5 degrees) close to an active delta channel proved diameters of up to 50 m (Figure 4-25). The main cracks seem to be perpendicular to the orientation of the water channel. It is assumed, that in general the cracks are relatively young because of their location in a Holocene river delta and their irregular, not well-formed shape. Further we can assume a surface, which is stable only during short timescales because of a changing delta setting and the repeated flooding with sediment accumulation or erosion events. The large size of polygons may depend on the large active layer depth of this coarse-grained and therefore well-drained material.

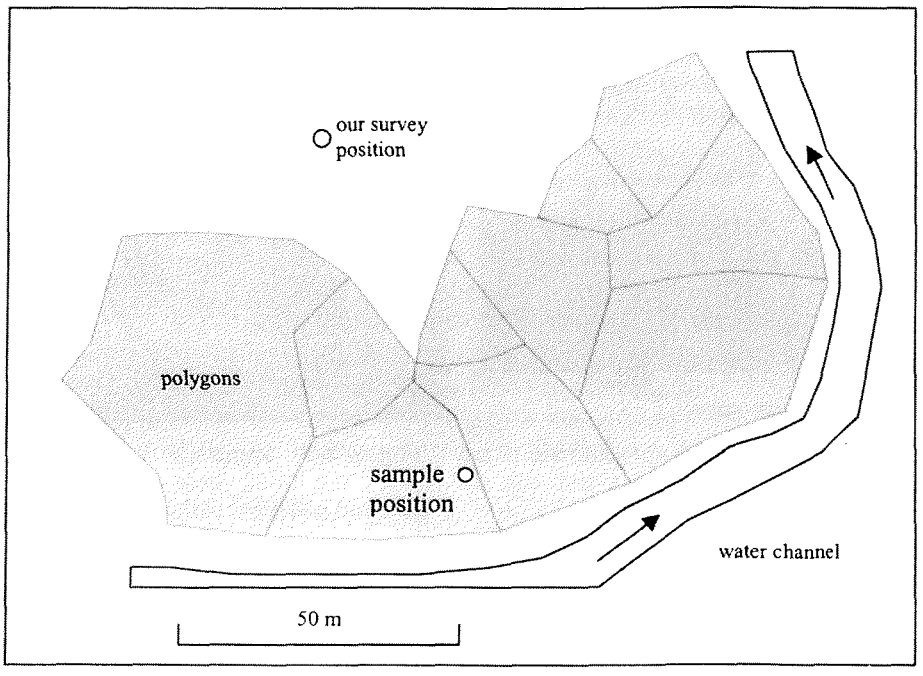

Figure 4-25: Survey of giant polygons in the old Khorogor delta

4.3. Ice Complex deposits at Neelov Bay

A cliff of about 2 to 5 m height forms the western coast of the Neelov Bay between the river mouth of Khatys Yuryakh and Khorogor. A profile of 3 m thick permafrost deposits with three ice wedge generations was studied here (Figure 4-26). The lower part of the profile down to the beach was buried by mud. A huge syngenetic ice wedge represents the first ice wedge generation. The head of this ice wedge is located about 1 m below the surface and has a width of 2.5 m. The root of the ice wedge seems to reach depths below sea level. A lot of pebbles and gravels were observed in the lateral contact zones of the ice wedge and the sediment. The ice is turbid and dirty with numerous mineral particles and air bubbles. The vertical striation is not clear. Seventeen samples of this ice wedge were taken from the left to the right with a distance of 12-15 cm (Khg-95-6). A thin vertical ice wedge with a width of 5-8 cm and a vertical size of 1.5 m represents a second generation. Its ice is clean and transparent and contains vertically oriented pebbles inside. The upper part of the ice wedge does not show any modern growth or frost cracks above and thus the ice wedge is not active. Three samples were taken from this ice wedge Khg-95-8. The third generation is represented by a thin hade ice wedge (Khg-95-6), which has intruded into the ice wedge of the first generation with an inclination of 30-40 degrees and a width of about 8 to 12 cm. Its milky-white ice intruded into the old ice wedge down to 1 m depth. It is an active ice wedge, since a modern frost crack was observed above. The sampling number of the ice wedge is Khg-95-8, and 3 samples of ice were taken.

The exposed permafrost deposits consist of a yellowish sandy loamy material with weakly subrounded pebbles (Ø 1 to 4 cm) and a lens-like cryostructure in the lowermost unburied part above beach-level. The following horizon is about 2 m thick and is composed of a mixture of gray silty fine-sand, weakly rounded pebbles and numerous smaller (Ø 1-5 cm) and larger (Ø 30 cm) peat inclusions. The upper horizon covers the large old ice wedge and consists of a frozen lower part with large peat lenses and a 0.5 m thick unfrozen part – the seasonal active layer. Altogether the conditions of this outcrop are pretty similar to the Late Pleistocene Ice Complex deposits studied in detail on the Bykovsky Peninsula further east (Mamontovy Khayata section, see chapter 4.5). Probably because of the nearby Kharaulakh Mountains the deposits are more coarse-grained at the Neelov Bay coast than at the eastern shore of Bykovsky Peninsula.

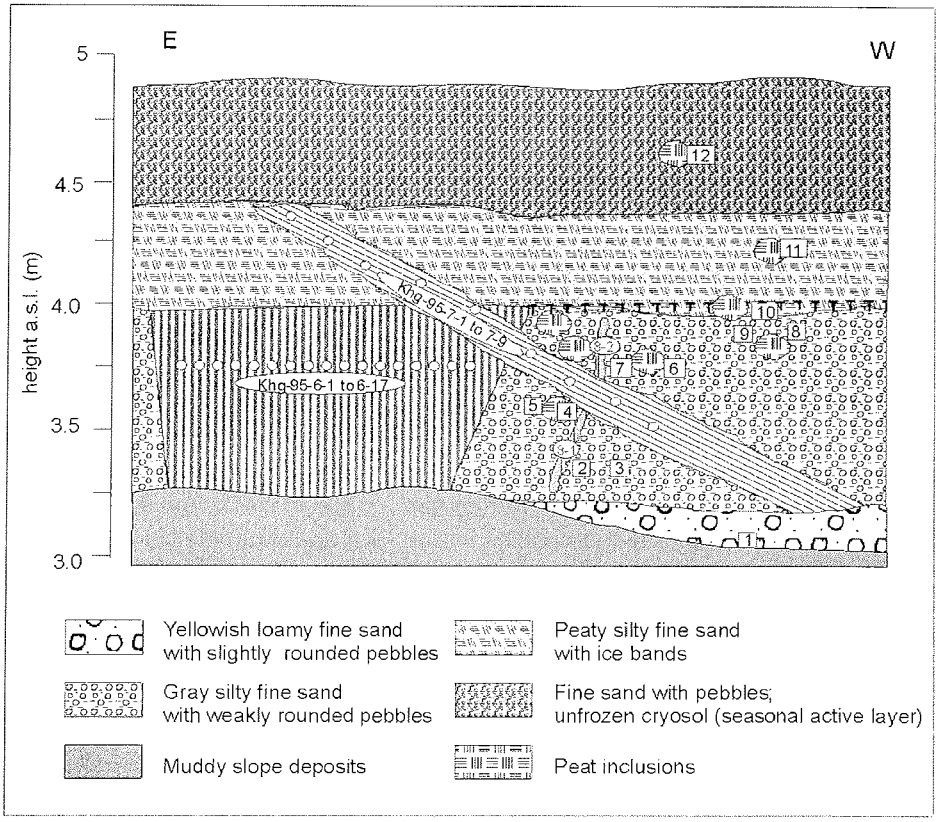

Figure 4-26: Profile Neb-1, Ice Complex outcrop at the Neelov Bay with ice wedges of various generations (Khg-95-6, Khg-95-7, Khg-95-8)

4.4. Nival processes and the periglacial / glacial (?) landscape in the region of Sevastyan Lake

The background for studying the area between Suononakh River, Sevastyan River and Sevastyan Lake were papers of Grosswald & Spektor (1993) and Grosswald (1998) describing traces of glacio-dislocations around Sevastyan Lake, drumlins and boulders scratched by glacial processes. We tried to re-investigate these very controversially discussed features. In addition, a perennial snowfield in the Sevastyan River valley and the periglacial landscape around the Sevastyan Lake were also part of our studies. The Sevastyan Lake is surrounded by a cuesta landscape (heights from 100-200 m a.s.l.) in the east, south and west. On the mountain slopes kar-like shapes with several 100 meters or some kilometres in diameter are visible, which might have been formed by perennial or seasonal snowfields or embryonic glaciers. The northern continuation of the Sevastyan Lake depression represents a large plain with several asymmetrical rocky hills of slate covered by weathered slate debris and large patches of rock debris which are almost free of vegetation (apart from a few lichens and mosses). The hard rock seems to be situated not very deep below these patches. The surface is dissected by sorted ground polygonal structures (large ones with 25 m and small ones with 3-5 m in Ø). The hills of slate ridges are common shapes in that plain. They are up to 10 to 15 m high but mostly they are much flatter (Figure 4-27). The general striking orientation is ENE-WSW like the valleys and ridges of the surrounding mountains. The permo-carboniferous basement cropping out here with slates and sandstones again is subject to subsidence within a tectonical graben structure (see Figure 4-2B).

Figure 4-27: Slate ridge in the Sevastyan plain (height ~15 m)

The orientation of the layer bedding, cleavage and shistosity of the slate ridges was measured at various sites in the region (Figure 4-28). These properties can be distinguished quite well and the way the are arranged to each othercould be a reason for the formation of the ridge-like shapes.

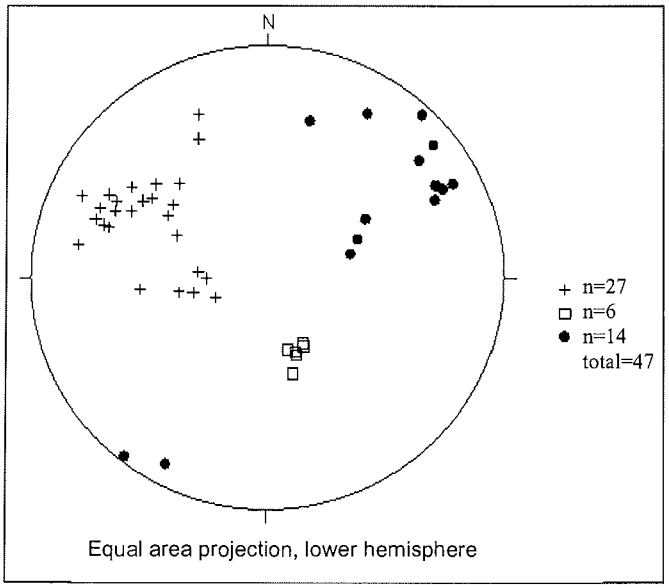

Figure 4-28: Schmidt's net of rock properties from the slate ridges in the Sevastyan area (plusses: shistosity, filled circles: cleavage, rectangles: sedimentary bedding)

The plain area north of the Sevastyan Lake is scarcely covered by vegetation (20-50 %). The surface is covered by weakly rounded debris of weathered sandstones and slates. Near the lake a zone of dense moss tundra is situated. The soil substrate mainly consists of silty sand with moderate debris content. Ice wedge polygons (Ø 15 to 20 m) and frost boils occur in that area. Chains of small ponds (Ø 10-15 m, 0.5-1 m deep) with interspaces of 20-25 m probably represent former small brooks flowing towards the lake. The lake water was sampled (Svy-96-2) as well as lake bottom sediment (Svy-2) and sediment from a frost boil (Svy-3).

A snowfield at the bank of the Sevastyan River was studied in detail. It was located at the southern inner bank of a river meander loop several 100 m before discharging into the Sevastyan plain (Figure 4-29 and 4-30). The site was well protected from direct sun insolation by steep rocks (~50 m above the river level) in the SE. More snowfields were noted in similar locations upstream. Polygons and thermokarst mounds were visible at the moderately inclined slope in the W above the snowfield reflecting relatively thick permafrost deposits. In higher positions above the moderate slopes only terraces covered by debris were formed. The snowfield had an extension of 350 m length, 10-100 m width and 2-2.5 m thickness. A mixture of plant detritus and silty sand densely covers the snow representing thaw residues of snow and wind transported material. These residues, named "chionoconite" according to Kunitsky et al. (2002) were also found in 1-2 cm thick covers on the pebble dominated valley bottom downstream and they reflect the largest extension of the snowfield.

The studied profile consists of about 0.1-0.5 m river ice in the lower part followed by 2 m well laminated firn-ice alternations with cross-bedding. Individual firn layers are up to 10 cm thick and ice layers about 1-2 cm. Densities between 0.76 and 0.84 g/cm^3 were measured from 3 different cubes of firn (Svy-1-4 to 1-6). A vertical profile in the snowfield was sampled for hydrochemical and isotope analysis (Svy-97-1 to 14). In order to study evaporation processes by stable isotope analysis about 1.5 mm snow was scraped off from one m^2 of the snow surface seven times and one reference sample in a depth of 5 cm (Svy-E1 to E-8). Additionally, Sevastyan River water (Svy-96-1) was sampled. More samples were taken from thaw residues of chionoconite (Svy-1-1, 1-2) and slope material above the snowfield (Svy 1/3).

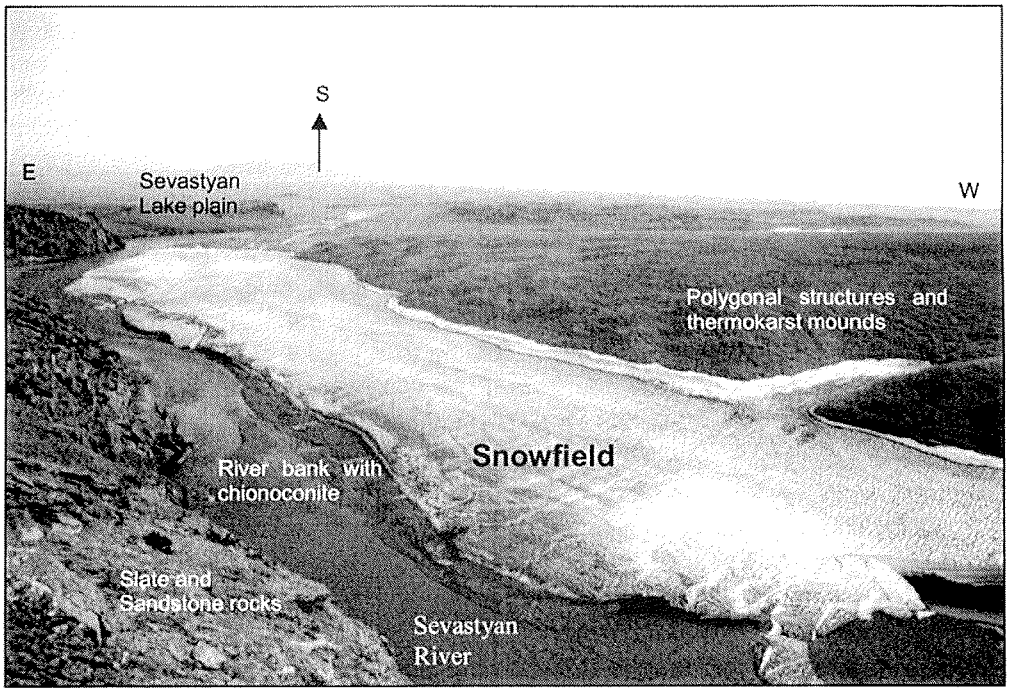

Figure 4-29: Snowfield in the Sevastyan River valley, view from N to S

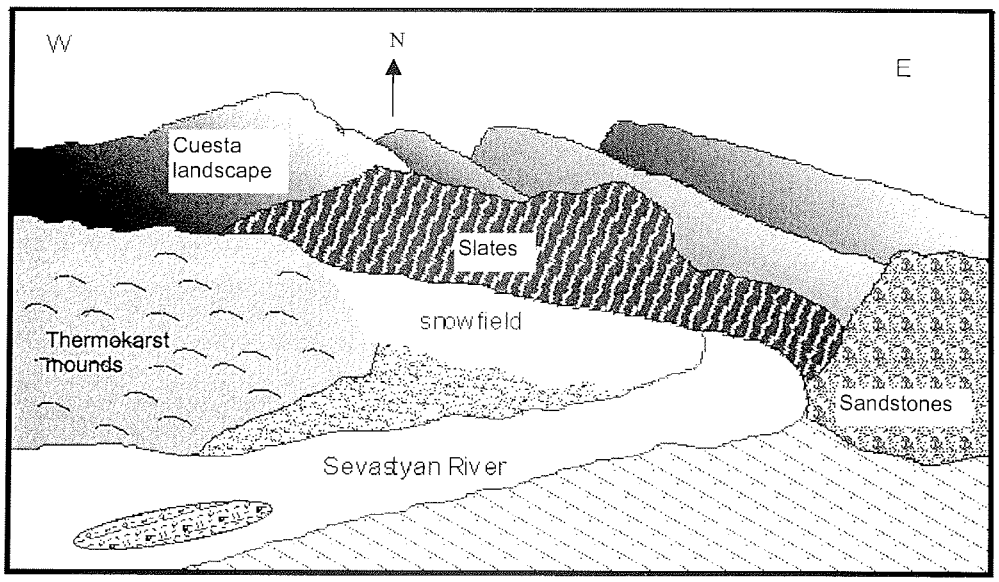

Figure 4-30: Scheme of the snowfield location and the surrounding geomorphological situation in the Sevastyan River valley, view from S to N

4.5 Periglacial processes and landscapes on Bykovsky Peninsula

4.5.1. Surface phenomenons on the southwestern Bykovsky Peninsula

In the southwest of the Bykovsky Peninsula a one day field trip was carried out to investigate the geomorphology and sedimentology of this possibly genetical link of the Khorogor Valley and the Ice Complex deposits of the peninsula. The field trip started at the most western point of the Safroneeva Lagoon at the southern shore of the peninsula. The east shore of the Safroneeva Lagoon as well as the north and south shores of the peninsula consist of cliffs of about 10-15 m height. The cliffs show formations of large thermokarst mounds, which are an indication for the former existence of large ice wedge polygons, hence ice-rich deposits. In general, the area consists of a gently rising plain towards the east from 15 to 40 m a.s.l.. Proceeding from an initial thermokarst depression in the central higher part of the region, the plain is separated by radial oriented thermo-erosional valleys (Figure 4-31).

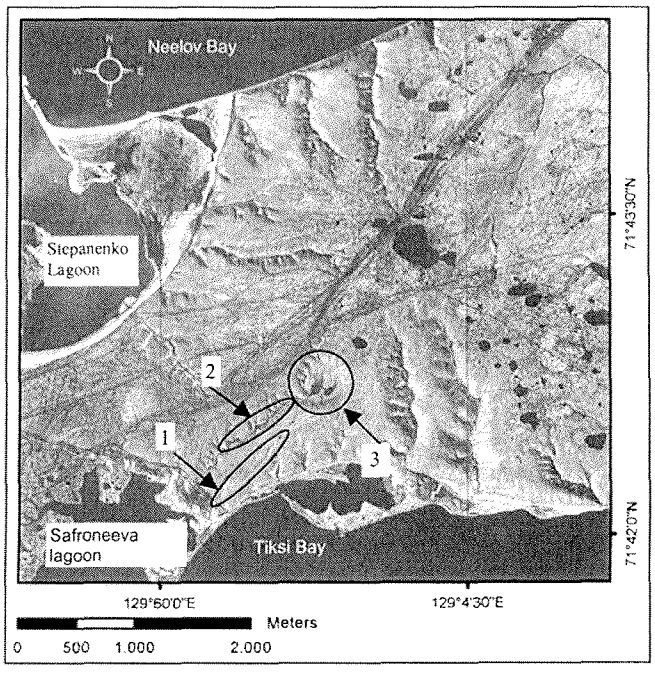

Figure 4-31: Study area on the SW Bykovsky Peninsula (CORONA image, July 1969)
1 Initial thermoerosional valley, 2 Large thermoerosional valley, 3 Small thermokarst

First an initial thermo-erosional valley was investigated. In the flat bottom of a gentle depression close to the coastal cliff a small erosional channel of about 1 m depth with running water has developed right above the ice wedge net (Figure 4-31). Large ice wedge polygons with 10-20 m in diameter were

observed there and several polygons were measured by tape. The generally wet depression was lowered by about 1 m compared to the surrounding surface and vegetated by mosses, few grasses and lichens. The running water from the channel flowed on the permafrost table (supra-permafrost water) down the slopes and represents mainly meteoric water. Sediment and ice samples were taken from an outcrop in the erosional channel (Kol-1, Kol-2-1 to 4, Kol-95-2-1 to 3)(Figure 4-32). Approximately 400 m north of this initial valley a large thermo-erosional valley was observed. The valley was lowered down 8-10 m below the surface forming a U-shaped valley with steep rims and a flat bottom. The wet bottom was densely covered by grass, in some places standing water of up to 10 cm depth was found. At the rims large thermokarst mounds had developed. The sizes and distances of some of them were measured by tape. The thermokarst mounds had diameters of about 7 m and heights of 4-6 m and they consist of silty sand with gravels (samples Kol-4-2, 4-3). The size of the former polygons was estimated with about 10-15 m in diameter.

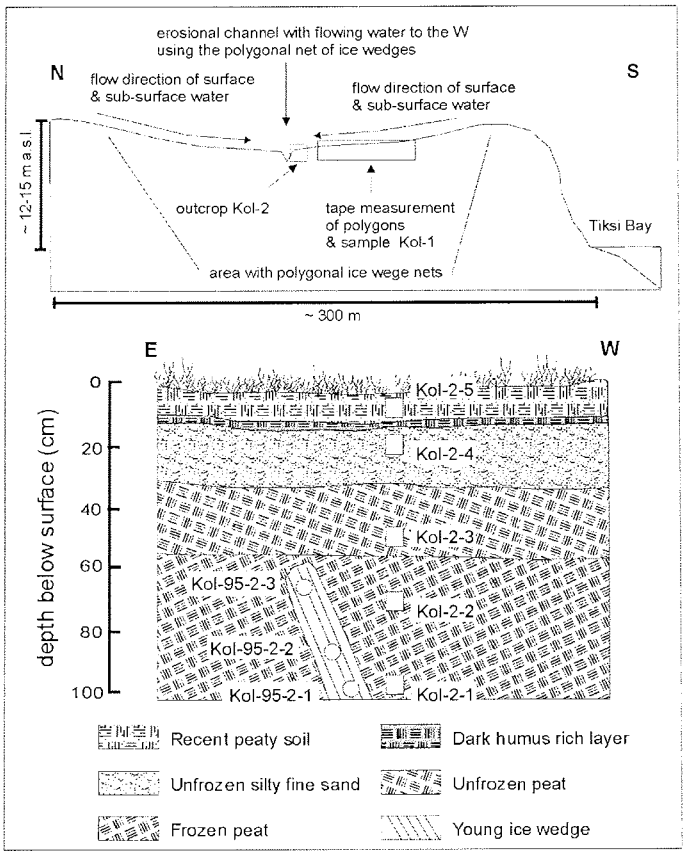

Figure 4-32: Cross-profile of the south shore of the western Bykovsky

This valley had its origin in a small circular thermokarst depression. The bottom of the depression was lowered approximately 10 m and 2 elongated lakes (110 x 55 m and 100 x 75 m) had developed therein (Figure 4-33). In the north a flat valley is discharging into the depression forming a gentle wet slope of silty fine sand covered with grass. On this slope flat terraces form steps of 10-30 cm, which may represent individual sedimentation and accumulation events produced by running water during the snow melt. Around the lakes very wet moss-grass tundra with rectangular, water-filled low-centre polygons was found. Compared to the western part the eastern part of the depression is raised several decimetres. The step is marked by silty sand rich in sandstone pebbles, which only occur in the eastern part (sample Kol 4-1). Several erosion channels separate the rim of the depression and thermokarst mounds have formed in the upper parts.

Outgoing from our landing point towards the small thermokarst depression we also examined several frost boils. In most of them we found more or small less rounded gravels (1 cm in ∅, sample Kol-3)). This indicates that layers with coarser grained material can be found right below the fine-grained, silty-sandy surface deposits.

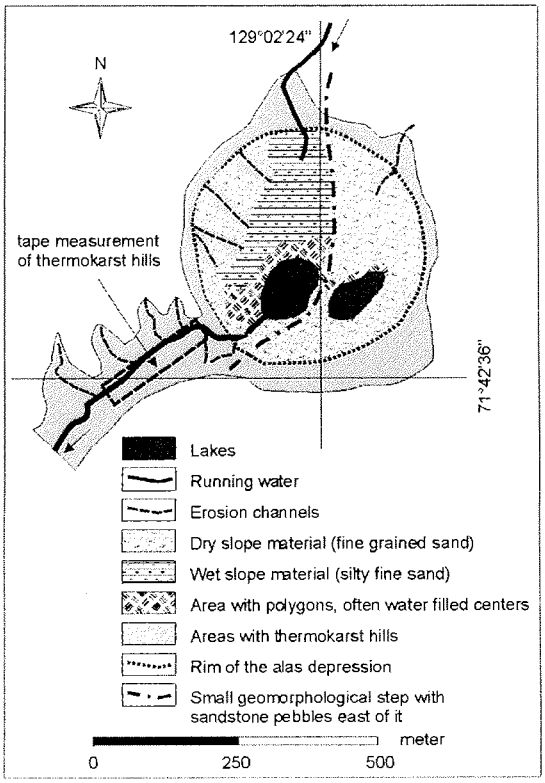

Figure 4-33: Scheme of the investigated thermokarst depression on the western Bykovsky Peninsula

4.5.2. Mamontovy Khayata section and the Mamontovy Bulgunyakh pingo

A most detailed profile of ice wedges was sampled for stable isotope analyses at Mamontovy Khayata outcrop on Bykovsky Peninsula (Figure 4-34). Sampling at this site started in 1998 (Meyer et al. 1999, ROPR 315), when an overview stable isotope record was gained between sea level and the top of the outcrop (Meyer, 2001, Meyer et al. 2002). In 2001, a group of Russian scientists refined the ice wedge sampling in the upper part of the outcrop at Mamontovy Khayata section (Sher et al. 2002). The main aim was to complete the stable isotope profile of ice wedges especially in that part of the section, which is assumed to be as old as or postdating the Late Glacial Maximum (LGM). It could not be sampled before for reasons of difficult outcrop conditions. Two horizontal ice wedge transects could be sampled in respective heights of 32 m and 29.5 m. Both heights correspond to a period predating the LGM, according to the age-height relationship published in Meyer et al. (2002) and Schirrmeister et al. (2001). Therefore, on September 4th 2002, a new attempt was undertaken to sample the LGM part of the profile in order to answer the question whether the winter temperatures were colder or warmer during the LGM than in the Kargin interstadial.

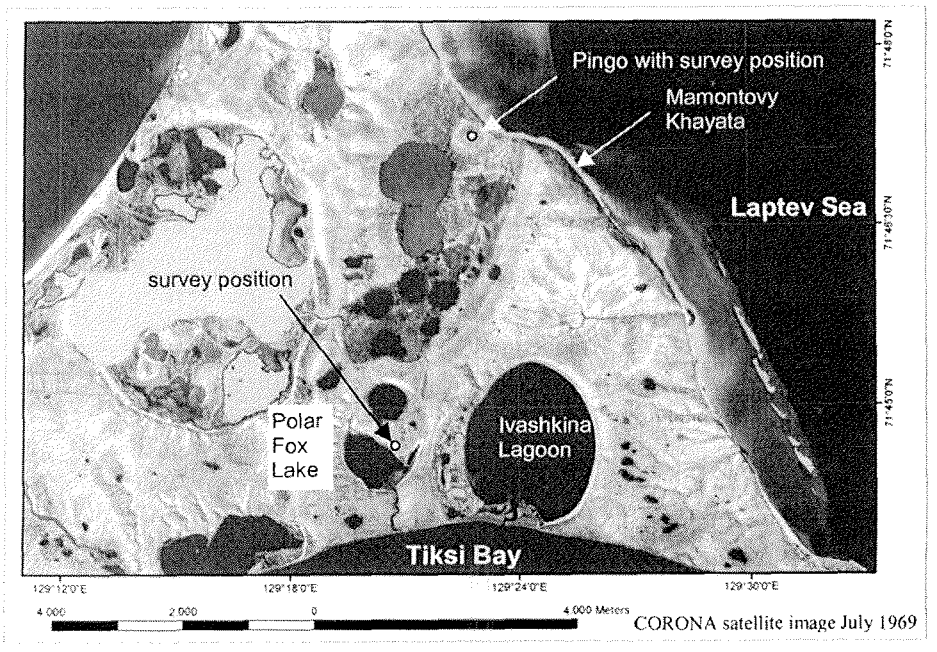

Figure 4-34: CORONA Satellite image of the SE region of the Bykovsky Peninsula

In 2002, the outcrop conditions allowed the sampling of the uppermost section assumed to be of LGM age. Ice wedge sampling was carried out (as described in more detail in chapter 3.9) for one horizontal sampling transect in a depth of 4.85 m below the surface and a depth of 4.5 m below the permafrost table (Figure 4-35). This means a height of about 34.5 m above sea level for the sampled profile, corresponding to about 14 ka BP ^{14}C age.

The selected ice wedge MKh-02 is characterised by clear, transparent and sometimes yellowish ice, with well-developed vertical structures such as 1 - 5 mm wide elementary ice veins and elongated gas bubbles (up to 8 mm long), especially on the left part of the wedge. Elementary ice veins might cross each other. The vertical structures are less well developed on the right part of the ice wedge, which also contains a relatively high amount of organic matter (e.g. lemming coprolites and plant fragments). In general, the content of mineral particles is low in the ice wedge, although some mineral veins of about 1 mm in width occur. A peculiarity was the finding of a fluid inclusion of ca. 6 mm in diameter in the ice.

The sediment column is covered by an active layer about 35 cm thick, and it is subdivided into two main units: in the upper 2 m of the profile (between 36.8 m and 38.8 m a.s.l.), the sediment surrounding the ice wedge is composed of ice-rich silty sand of greyish colour and a fine (above) to coarse (below) lens-like reticulate cryostructure interrupted by ice belts (Appendix 4-1). A horizon of peaty soil pockets of up to 40 cm separates the subunits of different cryostructure, and is inserted into the lower subunit.

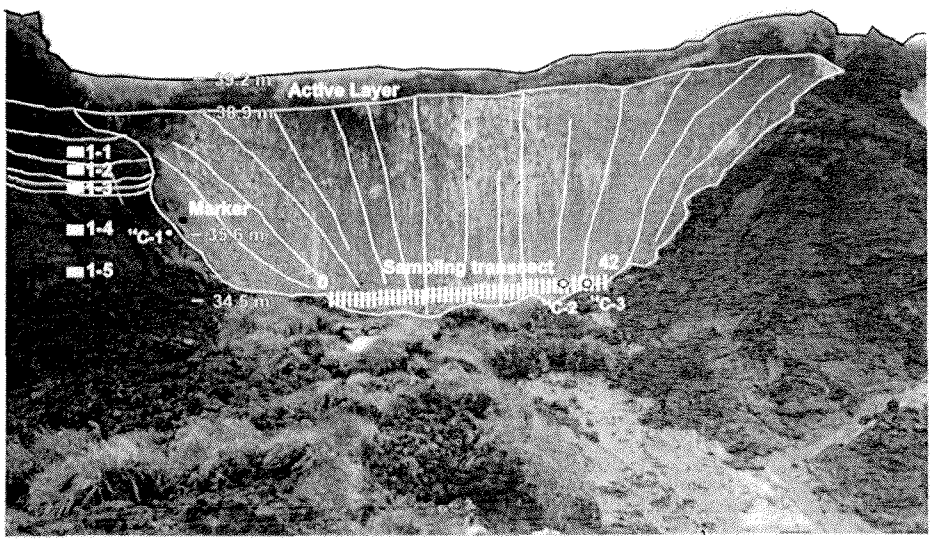

Figure 4-35: Ice wedge and sediment sequences below the top of Mamontovy Khayata section, Bykovsky Peninsula, profile Mkh-02 .

Below 36.8 m, the sediment consists of greenish-grey "loess-like" silty sand with massive cryostructure, cut by a few thin ice belts with a much lower ice content compared to the upper unit. From above, organic-rich cryoturbation pockets penetrate into this lower unit.

A small bone was found *in situ* at a height of 35.6 m in the sediment 5 cm beneath the left rim of the ice wedge, which may be used for an age estimate of the sediment. Two additional samples of datable organic matter could be found in the ice wedge at 3.55 m and 4.05 m of the left edge of the transect. Ice wedge samples were taken in 10 cm intervals by means of a chain saw with an approximate width of each ice sample varying between 1.5 and 2 cm. A total number of 43 samples were retrieved from the 4.35 m long horizontal sampling transect. The samples were sealed in plastic pockets and transported in frozen state to the AWI, where they will be measured for stable oxygen and hydrogen isotopic composition, using a Finnigan MAT Delta-*S* mass spectrometer.

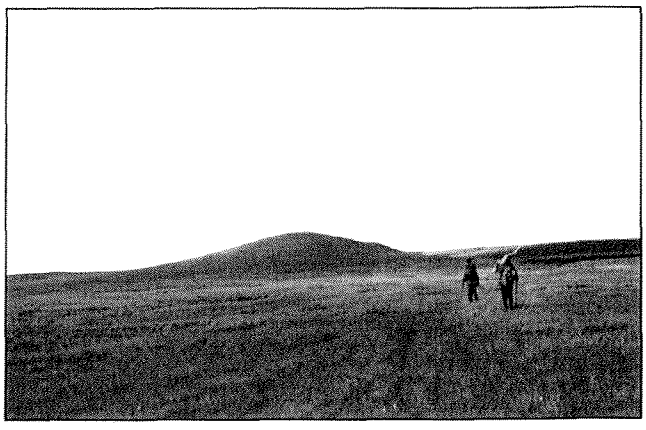

Figure 4-36: The pingo Mamontovy Bulgunnyakh within the thermokarst depression Mamontovy Bysagasa.

Pingos are very common in the NE Siberian lowlands as well as in Alaska, Canada, Sweden and Spitsbergen. In NE Siberia these structures are connected with thermokarst depressions and certain sedimentary and hydrological conditions. On the Bykovsky peninsula 4 pingos are known, of which Mamontovy Bulgunyakh is the second biggest with about 25 m a.s.l. and coverage of about 90.000 m^2. This pingo is situated within the thermokarst depression of Mamontovy Bysagasa close to the western shoreline of the peninsula and the Mamontovy Khayata outcrop in the SE (Figure 4-34 and Figure 4-36). It was subject to a drilling campaign in 1998 by the German-Russian expedition "Lena-Delta 1998" (Siegert et al., 1999).

The core drilling was stopped at a depth of about 6.5 m from top of the pingo when reaching the massive ice lens. The sediments consist mainly of silty sand with a low gravimetric ice content of 25-50 wt-% and an alternating cryostructure of horizontal, subvertical and diagonal lenses, massive structures and broken horizontal ice veins.

The pingo surface is covered by dry hummocky grass vegetation and is disturbed by solifluction. Several sediment fans occur at the pingo base and at a step at the eastern slope. This is caused by a nival niche, which obviously appears as a snowfield on some satellite pictures. The pingo outline was determined by the boundary to the wet tundra plain, which is characterized by brownish moss and peat vegetation as well as polygonal patterns.

The pingo is visible on high-resolution CORONA satellite images but its extent could not be determined, as there is no exact boundary to the surrounding areas. During this expedition the pingo was surveyed in detail by laser tachymetry. The survey was made from 2 survey positions on top of the pingo by measuring points along downslope transects. Altogether 27 transects with 213 data points were measured (Figure 4-37). Along 12 transects distributed over the pingo surface additionally 89 active layer depths were measured (Fig 4-38).

The absolute height of the pingo was determined with 25.57 ± 0.25 m a.s.l. according to the present sea level that day. This measurement has still to be corrected by water-depth gauge values obtained from the Tiksi Hydrometeorological Station.

Figure 4-37: Isoheights of the pingo Mamontovy Bulgunnyakh.

Figure 4-38: Active layer depths of the pingo Mamontovy Bulgunnyakh.

4.5.3. The Polar Fox Lake

The Polar Fox Lake is situated within a thermokarst depression at the south coast of the Bykovsky Peninsula (Figure 4-34). Some hundred meters to the east the large Ivashkina Lagoon is located in another thermokarst depression. The Polar Fox depression contains two large water bodies (> 200.000 m^2) and two small ones (< 30.000 m^2). The southern water body, which is the Polar Fox Lake in *sensu strictu*, is connected with the Tiksi Bay by an up to 8 m wide channel, which is a former thermo-erosional or dry valley (Figure 4-39). Therefore, the "lake" is actually a lagoon in a kind of a "pre-Ivashkina phase". On remote sensing images of different years (1951-1999) we could observe a change in the water level and the shoreline of the lake. On the shore some terraces with tree-trunks were deposited, originally transported into the depression by seawater or sea ice (Figure 4-40). The wood is partially strongly weathered and looks very old and sometimes it is deeply buried under peat and slope sediments. Thus we assume, that the sea influence has been active in the lagoon for at least several hundred years. Samples were taken from lake deposits (Ope 4 & 6), from surface material (Ope 5) as well as from lake water (Ope 1 to 3).

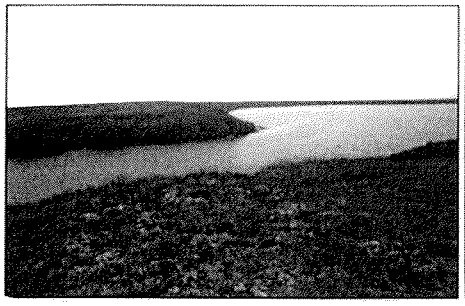

Figure 4-39: Mouth of the about 8 m wide channel from the Tiksi Bay into Polar Fox lake

Figure 4-40: Terraces of old tree-trunks at the eastern shore of Polar Fox Lake, sometimes already covered by slope deposits

The geodetic survey of the southern part of the depression was done from a single position on a flat central land bridge dividing the two large water bodies. We surveyed the shore of the Polar Fox lagoon and the upper rim of the depression. The shore survey represents the water level situation of that day. We have to verify these results by data of water-depth gauges for the Tiksi bay collected by the Tiksi Hydrometeorological Station. Even during our survey campaign the water level oscillated several dm forced by tidal and wind effects in the Tiksi bay. We registered changes in the water level of up to 60 cm relative to our survey position.

To illustrate the amount of sea level changes in that region and hence the influence on lake level changes, Figure 4-41 shows water level data from the gauge in Tiksi during July/August in 2000.

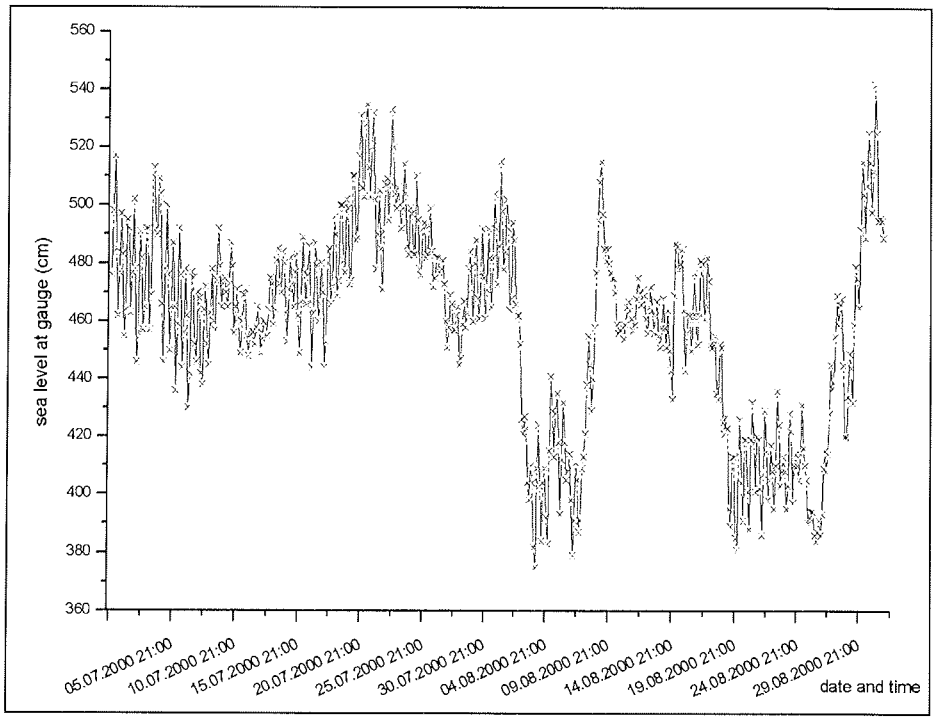

Figure 4-41: Data from the sea level gauge of the Hydrometeorological Station in Tiksi from July and August in 2000 (with friendly permission of A. Gukov).

As the graph shows, sea level changes during one day are moderate with 40-50 cm while sometimes changes of up to 150 cm within 24 hours are also possible. The sea level gauge of Tiksi is about 19 km far away from the investigation site.

The absolute height a.s.l. could not be determined in the field, because no trigonometric points were visible from the survey position within the depression, but after we had applied the tidal data to our measurements, we could interpolate a height above the sea level. Altogether we measured 120 points.

4.6. The snowfield at the "Stolovaya Gora" – a potential nival monitoring area

Nival processes connected with snowfields shape the modern as well as the past Arctic landscape at larger scales. Therefore, to understand the landscape development here, detailed monitoring and measurement of various parameters influencing nival processes or resulting from them are necessary. One task of our studies was the selection of a future nival monitoring area near Tiksi, which has to be easily reached and observed. Such a site was obviously found at the southeast slope of the southern flank of Stolovaya Gora hill below the Diring-Kyuel Lake near Tiksi. The Stolovaya Gora hill ("Table Mountain") is characterized by a large nival kar at its eastern slope, which is well visible from Tiksi. Perennial snowfields occur in some hundred meter long narrow ravines down-cutting the slope as well as on nival steps and kars parallel to the contour lines at ca. 200 m a.s.l. (Figure 4-42).

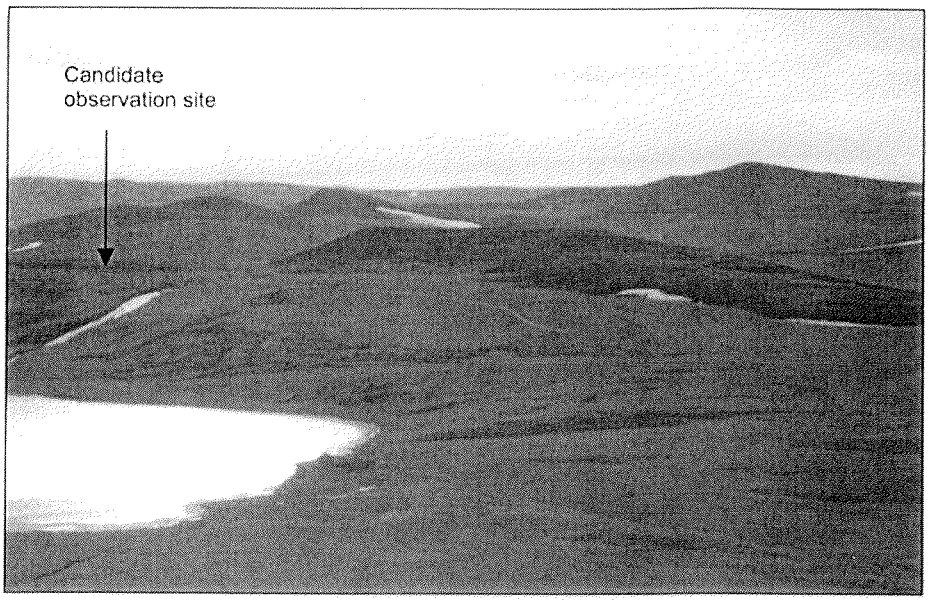

Figure 4-42: Snow fields at the south-eastern slope of the Stolovaya Gora hill south-flank above the Diring-Kyuel Lake (photo from summer 1998)

Below the top of the slope a steep and long edge of about 3 m in height was found consisting of dry rock-debris covered by lichens (Figure 4-43). Below this edge a gently inclined slope area spreads with one-meter broad streaks of rock debris with vegetation alternating each other (striped sorted ground). These stripes disperse into several frost boils and puddles (water sample Svy-96-11) in a wet nival meadow by a very small slope inclination. Below this terrace the slope is subdivided into three sections. The upper slope shows a grass surface torn up by solifluction, whereas at the lower slope the grass cover is compressed to solifluction terraces of about one meter height. Ice wedge polygons were formed at the lowermost flat part of the slope.

This year a snowfield was preserved within an up to 7 meters deep and ca. 400 m long erosional trench. Most likely this trench was filled with snow up to the top during winter. Actually the snow thickness on August 9th was less than one meter and only an area of about 150 x 5-10 m was covered by snow.

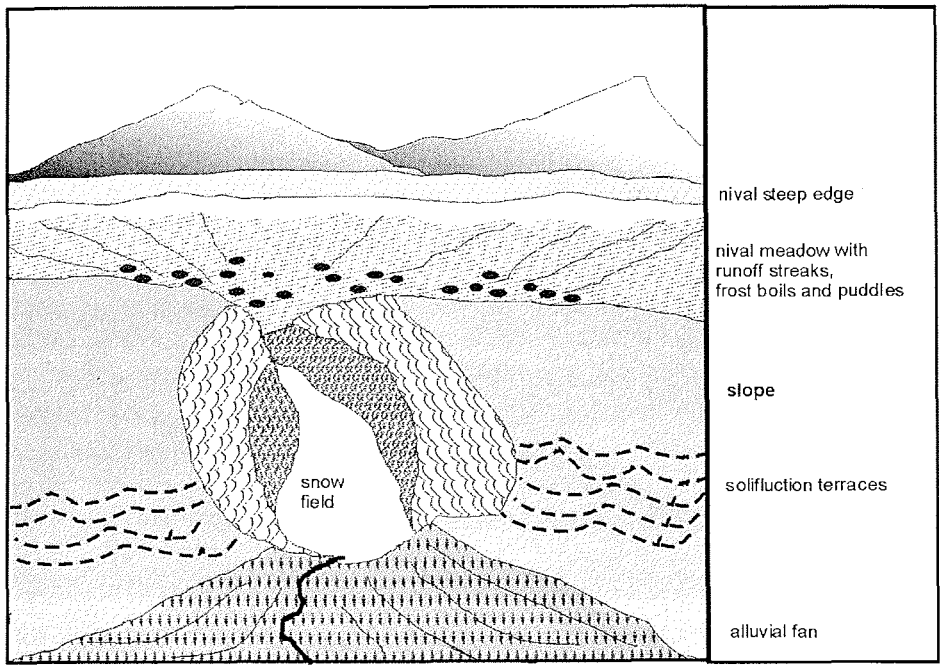

Figure 4-43: Schematic view on the candidate monitoring site for the snow field at the Stolovaya Gora hill.

The snow was sampled in a vertical profile with interspaces of 10 cm (Svy-97-15 to 23 (Figure 4-44). Chionoconite (mixture of organic and fine-grained sediment material) covers the snow (samples Stg-1-1, 1-3) as well as the surrounding rock debris and the trench slopes up to heights of 5 m. The stones at the bottom are obviously slightly rounded by running water (sample Stg-1-4). Individual boulders have diameters up to one meter. Linear surface patterns on

such boulders are stratification structures of sandstones cleared out by weathering. There were no traces of glacier movement at all. The slope material exposed at the steep wall of the trench contains slate debris and fine-grained material (sample Stg-1-2). The nival trench ends up with an alluvial cone and a small melt-water runoff brook (sample Svy-96-13) into lake Diring-Kyuel (sample Svy-96-14).

The idea for future studies of nival processes is the installation of measurement equipment within the central part of the snowfield for measuring snow thickness, temperatures in various depths, as well as above and below the snow cover, and other meteorological data (direction and force of wind, insolation, precipitation). Additional measurement equipment could be installed in the surrounding area in order to record more data like soil temperature and moisture. A regular monitoring of melt-water runoff rates and sediment discharge and the changes in snowfield extension and the slope morphology should be made as well as a regular sampling of snow, meltwater and sediments. For such investigations a detailed digital topographic model is necessary. If we manage to establish such a nival monitoring field it would enable us to determine more exactly the dependency of nival landscape morphology from climate parameters as well as balancing various influencing factors like snow volume, melt-water rates and sediment transport.

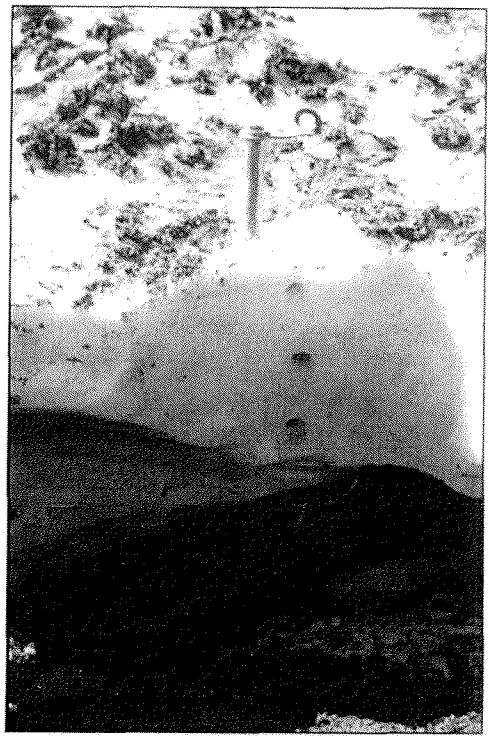

Figure 4-44: Photo of snowfield cross-section and the uppermost sample points

4.7 Appendices

Appendix 4-1. List of sediment samples collected around Tiksi.

	Sample description			Position						
No.	**Sample**	**Sedimentology**	**Cryolithology, ice content abs./grav. [wt %]**	**N 71°**	**E 128°**	**H NN (m)**	**Depth (m)**	**Remarks**	**Date**	**Ice/water samples**
1	Khg-1	Silty fine sand, single stones (weakly subrounded 2-7 cm)	Active layer	38.35	36.18		0	Frost boil Ø 0.6 m, station of transportable surface probe (TSP)	01.08.	
2	Khg-2	Sandstone		38.10	35.37		0			
3	Khg-3	Slate					0	Rocky ridge	01.08.	
4	Khg-4-1	Dolerit				ca. 190	0			
5	Khg-4-2	Dolerit				ca. 190	0			
6	Khg-5-1	Silty fine sand, single stones (2-7 cm)	Active layer (centre: 0.45 m, edge: 0.3-0.4 m)	39.9	33.00		0	Frost boil Ø 35 cm, v	01.08.	
7	Khg-5-2	Dark coarse-grained river sand		39.19	33.45			Khorogor River	01.08.	KHG-96-1
8	Khg-6	Silty fine sand	Active layer (centre: 0.52 m, edge: 0.35 m)	38.80	33.97		0	Frost boil Ø 70 cm, station of TSP	01.08.	
9	Khg-7	Brownish-gray, organic-rich, fine sand	Active layer (0.4 m)	38.39	35.27		15	Ice wedge (0.10-0.15 m) polygon (Ø 15 m) with recent frost fissures and frost boils (Ø 0.6-0.9 m)	01.08.	KHG-95-1
10	Khg-8-1	Silty sand	Transition layer, lens like structures	42.12	42.44		25	Emergency airstrip of an old airport	02.08.	KHG-96-3
11	Khg-8-2	Peat, brownish, weakly decomposed					0.15-0.20	Station of TSP		KHG-98-2
12	Khg-8-3	Moss				50	0-0.05	Large moss pad (40 x 17 m with polygons Ø 9 m)		KHG-96-4

Appendix 4-1. continuation.

Sample description				Position						
No.	**Sample**	**Sedimentology**	**Cryolithology, ice content abs./grav. [wt %]**	**N 71°**	**E 128°**	**H NN (m)**	**Depth (m)**	**Remarks**	**Date**	**Ice/water samples**
13	Khg-9-1	Silty sand	Active layer (0.55 m)	42.13	42.11		0	Moss pad (15 x 30 m) with frost boil (Ø 1.5 cm)	02.08.	
14	Khg-9-2	Gravel, weakly subrounded					0	Frost boil		
15	Khg-10-1	Slate		40.92	36.87	68.5	0		02.08.	
16	Khg-10-2	Fine-grained quartzitic sandstone		40.92	36.87		0			
17	Khg-10-3	Lake deposit		40.92	36.87			Figurnoe Lake, 0.5 m water depth, 3 m from the bank		KHG-96-5
18	Khg-10-4	Gravel, slates and sandstones, subrounded		40.92	37.47		0	Alluvial deposits		
19	Khg-10-5	Soil and gravels		40.92	37.47	75	0	Alluvial deposits		
20	Khg-10-6	Fine-grained quarzitic sandstone		40.97	37.74		0	Gravel plain		
21	Khg-11-1	Peat	Unfrozen, active layer 0.37-0.40 m	41.79	45.96		0.10-0.15	Station of TSP	02.08.	
22	Khg-11-2	Peat	Frozen				0.50-0.60	Thermokarst mound		
23	Khg-11-3	Peat	Frozen				0.75-0.85	(baydzherakh)		
24	Khg-12-1	Fluvial gravel		41.80	47.57			Khorogor River	02.08.	KHG-95-2
25	Khg-12-2	River sand								
26	Khg-13-1	Silty sand	Coarse lens-like structures, lower-most part of the seasonal active layer	44.01	43.17		0.27-0.33	Pit on the surface of an ice wedge polygon	03.08.	KHG-95-3
27	Khg-13-2	Moss peat					0.12-0.19			KHG-95-4
28	Khg-13-3	Moos					0-0.03			KHG-95-5

Appendix 4-1. continuation.

	Sample description			Position						
No.	**Sample**	**Sedimentology**	**Cryolithology, ice content abs./grav. [wt %]**	**N 71°**	**E 128°**	**H NN (m)**	**Depth (m)**	**Remarks**	**Date**	**Ice/water samples**
29	Khg-14-1	Water moss (Drepanocladus)		44.08	45.14	18.5		Flat (0.2-0.5 m depth) lake	03.08.	
30	Khg-14-2	Lake deposit					0.5	10 m from the bank		KHG-96-6
31	Khg-15-1	Silty fine sand, single stones	Active layer (centre: 0.50 m, edge: 0.25 m)	44.51	45.16		0	Frost boil (Ø 0.60 m)	03.08.	
32	Khg-15-2	Gravels, partly subrounded					0	Fluvial alluvium		
33	Khg-16-1	River sand		44.897	45.534			Khatis-Yuryakh River	03.08.	KHG-96-7
34	Khg-16-2	Fluvial gravel								
35	Khg-17-1	Silty fine sand		45.042	45.782		2.80	Thermokarst mound	03.08.	
36	Khg-17-2	with peat	small ice lines				2.60	(baydzherakh)		
37	Khg-17-3	inclusions					2.40			
38	Khg-17-4						2.20			
39	Khg-17-5						2.00			
40	Khg-17-6						1.80			
41	Khg-17-7						1.60			
42	Khg-17-8						1.40			
43	Khg-17-9						1.20			
44	Khg-17-10						1.00			
45	Khg-17-11						0.80			
46	Khg-17-12						0.60	Station of TSP on the surface		

Appendix 4-1. continuation.

Sample description				Position						
No.	**Sample**	**Sedimentology**	**Cryolithology, ice content abs./grav. [wt %]**	**N 71°**	**E 128°**	**H NN (m)**	**Depth (m)**	**Remarks**	**Date**	**Ice/water samples**
47	Svy-1-1	Plant remains, silty sand		33.917	44.848		0	Chionoconit, fresh from the snow field surface	04.08.	river water Svy-96-1
48	Svy-1-2	Plant remains, silty sand					0	Chionoconit layer, dry, 1 cm thick		surface SVY-97-E1 to 97-E-8
49	Svy-1-3	Silty fine sand						Below the snow field		
50	Svy-1-4		Ice cube				0.60-0.70	Above the Sevastyan river		SVY-97-1 to 97-14
51	Svy-1-5		Ice cube				0.80-1.00			
52	Svy-1-6		Ice cube				1.40-1.50			
53	Svy-2	Lake deposit		32.497	49.275		1 m water depth	Sevastyan lake	04.08.	SVY-96-2
54	Svy-3	Silty fine sand, grus					0	Frost boil	04.08.	
55	Neb-1-1	Loamy fine sand, gravels	Ice rich (46.9 / 88.3 %)	44.789	50.855	2.10	2.90	Coastal section at the Neelov Bay	05.08.	KHG-95-6
56	Neb-1-2	Dark brown peat, weakly decomposed	Frozen			2.60	2.40	Peat inclusion (Ø 0.05 m), for dating		to KHG-95-8
57	Neb-1-3	Greyish silty fine sand, gravels	Ice rich (47.4 / 90.0 %)			2.60	2.40			
58	Neb-1-4	Brown peat, weakly decomposed	Ice rich			3.20	1.80	Peat inclusion (Ø 0.30 m), for dating		
59	Neb-1-5	Greyish silty fine sand, gravels	Very ice rich (64.9 / 182.2 %)			3.20	1.80			
60	Neb-1-6	Brown peat, weakly decomposed	Very ice rich			3.45-3.55	1.45-1.55	Peat inclusion (Ø 0.20 - 0.30 m), for dating		
61	Neb-1-7	Greyish silty fine sand, gravels	Very ice rich (55.5 / 124.6 %)			3.35-3.45	1.55-1.65			

Appendix 4-1, continuation.

	Sample description			Position						
No.	**Sample**	**Sedimentology**	**Cryolithology, ice content abs./grav. [wt %]**	**N 71°**	**E 128°**	**H NN (m)**	**Depth (m)**	**Remarks**	**Date**	**Ice/water samples**
62	Neb-1-8	Brown peat, weakly decomposed	Very ice rich			4.00-4.10	0.90-0.100	Peat inclusion (Ø 0.05m), for dating		
63	Neb-1-9	Greyish silty fine sand, gravels	Very ice rich (60.1 / 150.9 %)			3.90-4.00	1.00-1.10			
64	Neb-1-10	Peaty silty fine sand, gravels	Very ice rich (70.1 / 234.0 %)			4.20	0.80	Thermokarst mound		
65	Neb-1-11	Peat, brown, fresh	Unfrozen			4.50	0.50	For dating		
66	Neb-1-12	Sandy soil	Uppermost part of the active layer			4.90	0.10			
67	Neb-1-13	Gravels				2.10-4.90	0.10-2.90	Mixture by the whole profile		
68	Khg-18-1	Coarse sand, gravels		42.196	57.794		0.5-0.6	Pit in the old Khorogor river delta	06.08.	
69	Khg-18-2	Fluvial gravel					0.1-0.2			
70	Khg-19-1	Gravel		38.524	34.324	ca. 116	0	Terrace F, Top	07.08.	
71	Khg-19-2	Loamy fine sand		38.617	34.581	ca. 108	0	Terrace F		KHG-95-9 to 11
72	Khg-19-3	Silty fine sand, gravels		38,580	34.832	ca. 98		Between terraces F-D		KHG-98-4
73	Khg-19-4	Silty fine sand		38.573	35.048	ca. 90	0.15	Between terraces E-D		
74	Khg-19-5	Plant detritus, fine sand		38.515	35.386	ca. 84	0	Chionoconit, Terrace D		KHG-96-9 to 10
75	Khg-19-6	Gravels, subrounded (0.1-0.2 m)		38.515	35.386	ca. 84	0	Terrace D		
76	Khg-19-7	Silty fine sand, single gravels		38.480	36.065	ca. 82	0.10	Frost boil (Ø 0.60 m) between terraces C-B		
77	Khg-20-1	Silty fine sand, gravels	Frozen	38.412	36.500	ca. 80	0.40	Frost boil (Ø 0.50 m)	09.08.	
78	Khg-20-2	Dark gray silty fine sand, loamy	Unfrozen				0.10	Active layer 0.21 to 0.35 m thick		ground-water

Appendix 4-1. continuation.

No.	Sample	Sample description: Sedimentology	Cryolithology, ice content abs./grav. [wt %]	Position: N 71°	E 128°	H NN (m)	Depth (m)	Remarks	Date	Ice/water samples
79	Stg-1-1	Plant remains, fine sand		36.645	46.106		0	Chionoconit from snowfield surface near the Stolovaya Gora hill	10.08.	SVY-96-11 to 14
80	Stg-1-2	Silty fine sand, gravels					0	Slop material		SVY-97-15 to 23
81	Stg-1-3	Plant remains, fine sand					0.10	Chionoconit from snowfield surface		
82	Stg-1-4	Subrounded gravels, sandstone, quartz					0			
83	Kol-1-1	Peaty soil		42.326	01.236		0-0.05	Ice wedge polygon	11.08.	KOL-95-1
84	Kol-1-2	Silty fine sand					0.15	Western Bykovsky Peninsula		
85	Kol-2-1	Peat	Frozen	42.338	01.299		1.00	Western Bykovsky Peninsula	11.08.	KOL-95-2
86	Kol-2-2	Peat	Frozen				0.70			
87	Kol-2-3	Peat	Unfrozen, active layer 0.45 m				0.50			
88	Kol-2-4	Silty fine sand	Unfrozen				0.20			
89	Kol-2-5	Peaty soil					0.10	Surface		
90	Kol-3	Subrounded gravels		42.514				Sampled on the surface of various frost boils	11.08.	
91	Kol-4-1	Subrounded gravels, sandstone								
92	Kol-4-2	Subrounded gravels		42.710	02.215					
93	Kol-4-3			42.710	02.215					

Appendix 4-1. continuation.

	Sample description			Position						
No.	**Sample**	**Sedimentology**	**Cryolithology, ice content abs./grav. [wt %]**	**N 71°**	**E 128°**	**H NN (m)**	**Depth (m)**	**Remarks Mamontovy Khayata**	**Date**	**Ice/water samples**
94	MKh-02-1-1	Silty fine sand	Ice rich, fine lens like reticulated, ice bands				1.65	Thermokarst mound	05.09.	MKH-02-1. 1 to 42
95	MKh-02-1-2	Cryoturbated peaty soil, peat pockets	Ice rich, coarse lens like reticulated				2.15		05.09.	
96	MKh-02-1-3	Silty fine sand, green-brownish, cryoturbated, peat pockets,	Ice poor, ice bands				2.75		05.09.	
97	MKh-02-1-4	Silty fine sand, grey, wood remains, small grass roots	Ice poor				3.05		05.09.	
98	MKh-02-1-5	Silty fine sand, grey, wood remains, small grass roots					5.25		05.09.	

No.	**Sample**	**Sedimentology**	**Cryolithology, ice content abs./grav. [wt %]**	**N 71°**	**E 129°**	**H NN (m)**	**Depth (m)**	**Polar fox lake (Ozera Petsa)**	**Date**	**Ice/water samples**
99	Ope-4	Middle-grained sand		44.696	20.784			Beach sand	06.09.	OPE-1 to 3
100	Ope-5	Silty sand + gravel		44.696	20.784			Surface sample, frost boil	06.09.	
101	Ope-6	Middle-grained sand		44.696	20.784			Beach sand	06.09.	

Appendix 4-2. List of ice, water and snow samples collected around Tiksi.

No.	Date	Sample	Type	Isotopes ^{18}O	Isotopes ^{2}H	^{3}H	Anion/ cation	Remarks
1	31.07.	TIK 99-1	RW	X	X	X	-	
2	01.08.	KHG 96-1	SW	X	X	X	-	Khorogor River
3	01.08.	KHG 95-1	RIW	X	X	X	X	Recent ice wedge
4	01.08.	KHG 96-2	SW	X	X	X	-	Vassily River
5	02.08.	KHG 96-3	SW	X	X	-	-	Pond Khorogor Valley
6	02.08.	KHG 98-1	GW	X	X	-	-	
7	02.08.	KHG 96-4	SW	X	X	X	-	Pond Khorogor Valley
8	02.08.	KHG 98-2	GW	X	X	-	-	
9	02.08.	KHG 99-2	RW	X	X	X	-	
10	02.08.	KHG 96-5	SW	X	X	X	-	Figurnoe lake
11	02.08.	KHG 95-2	RIW	X	X	X	X	Khorogor River, point 8
12	03.08.	KHG 96-6	SW	X	X	X	-	unnamed lake
13	03.08.	KHG 96-7	SW	X	X	X	-	Khatys Yuryakh River
14	03.08.	KHG 96-8	SW	X	X	X	-	Neelov Bay
15	03.08.	KHG 95-3	RIW	X	X	X	X	Head
16	03.08.	KHG 95-4	RIW	X	X	X	X	Head
17	03.08.	KHG 95-5	RIW	X	X	X	-	Head
18	04.08.	SVY 96-1	SW	X	X	X	-	Sevasyan Yurege River
19	04.08.	SVY 97-1	SP	X	X	X	-	Bottom of snowfield
20	04.08.	SVY 97-2	SP	X	X	X	-	
21	04.08.	SVY 97-3	SP	X	X	X	-	
22	04.08.	SVY 97-4	SP	X	X	X	-	
23	04.08.	SVY 97-5	SP	X	X	X	-	
24	04.08.	SVY 97-6	SP	X	X	X	-	
25	04.08.	SVY 97-7	SP	X	X	X	-	
26	04.08.	SVY 97-8	SP	X	X	X	-	
27	04.08.	SVY 97-9	SP	X	X	X	-	
28	04.08.	SVY 97-10	SP	X	X	X	-	
29	04.08.	SVY 97-11	SP	X	X	X	-	
30	04.08.	SVY 97-12	SP	X	X	X	-	
31	04.08.	SVY 97-13	SP	X	X	X	-	
32	04.08.	SVY 97-14	SP	X	X	X	-	Top of snow field
33	04.08.	SVY 97-E1	SP	X	X	X	-	Evaporation experiment
34	04.08.	SVY 97-E2	SP	X	X	X	-	
35	04.08.	SVY 97-E3	SP	X	X	X	-	
36	04.08.	SVY 97-E4	SP	X	X	X	-	
37	04.08.	SVY 97-E5	SP	X	X	X	-	
38	04.08.	SVY 97-E6	SP	X	X	X	-	
39	04.08.	SVY 97-E7	SP	X	X	X	-	
40	04.08.	SVY 97-E8	SP	X	X	-	-	
41	04.08.	SVY 96-2	SW	X	X	X	-	Sevastyan Lake

Appendix 4-2. continuation.

No.	Date	Sample	Type	^{18}O	^{2}H	^{3}H	Anion/ cation	Remarks
42	05.08.	KHG 95-6-1	IW	X	X	X	-	Ice Complex
43	05.08.	KHG 95-6-2	IW	X	X	X	-	Neelov Bay
44	05.08.	KHG 95-6-3	IW	X	X	-	-	
45	05.08.	KHG 95-6-4	IW	X	X	-	-	
46	05.08.	KHG 95-6-5	IW	X	X	-	-	
47	05.08.	KHG 95-6-6	IW	X	X	-	-	
48	05.08.	KHG 95-6-7	IW	X	X	X	-	
49	05.08.	KHG 95-6-8	IW	X	X	-	-	
50	05.08.	KHG 95-6-9	IW	X	X	-	-	
51	05.08.	KHG 95-6-10	IW	X	X	X	-	
52	05.08.	KHG 95-6-11	IW	X	X	-	-	
53	05.08.	KHG 95-6-12	IW	X	X	-	-	
54	05.08.	KHG 95-6-13	IW	X	X	-	-	
55	05.08.	KHG 95-6-14	IW	X	X	-	-	
56	05.08.	KHG 95-6-15	IW	X	X	-	-	
57	05.08.	KHG 95-6-16	IW	X	X	-	-	
58	05.08.	KHG 95-6-17	IW	X	X	-	-	
59	05.08.	KHG 95-7-1	IW	X	X	X	-	Holocene
60	05.08.	KHG 95-7-2	IW	X	X	X	-	Holocene
61	05.08.	KHG 95-7-3	IW	X	X	X	-	Holocene
62	05.08.	KHG 95-7-4	IW	X	X	X	-	Holocene
63	05.08.	KHG 95-7-5	IW	X	X	X	-	Holocene
64	05.08.	KHG 95-7-6	IW	X	X	X	-	Holocene
65	05.08.	KHG 95-7-7	IW	X	X	X	-	Holocene
66	05.08.	KHG 95-7-8	IW	X	X	X	-	Holocene
67	05.08.	KHG 95-7-9	IW	X	X	X	-	Holocene
68	05.08.	KHG 95-8-1	IW	X	X	X	-	Holocene/modern ice wedge
69	05.08.	KHG 95-8-2	IW	X	X	X	-	Holocene/modern ice wedge
70	06.08.	TIK 99-3	RW	X	X	X	-	
71	07.08.	KHG 95-9	RIW	X	X	X	-	
72	07.08.	KHG 95-10	RIW	X	X	X	-	
73	07.08.	KHG 95-11	RIW	X	X	X	-	
74	07.08.	KHG 95-12	TI	X	X	X	-	Segregated ice/ice lens
75	07.08.	KHG 98-3	GW	X	X	X	-	
76	07.08.	KHG 98-4	GW	X	X	X	-	
77	07.08.	KHG 96-9	SW	X	X	X	-	
78	07.08.	KHG 96-10	SW	X	X	X	-	
79	09.08.	KHG 98-5	GW	X	X	X	-	Vasili valley (point 2)
80	10.08.	TIK 99-4	RW	X	X	X	-	
81	10.08.	SVY 96-11	SW	X	X	X	-	Stolovoya Gora hill Terrace near snow field
82	10.08.	SVY 96-12	SW	X	X	X	-	Upper part of snow field (stream)
83	10.08.	SVY 96-13	SW	X	X	X	-	Bottom part of snow field (stream)
84	10.08.	SVY 97-15	SP	X	X	X	-	Snow field
85	10.08.	SVY 97-16	SP	X	X	X	-	Snow field
86	10.08.	SVY 97-17	SP	X	X	X	-	Snow field
87	10.08.	SVY 97-18	SP	X	X	X	-	Snow field
88	10.08.	SVY 97-19	SP	X	X	X	-	Snow field

Appendix 4-2. continuation.

No.	Date	Sample	Type	^{18}O	^{2}H	^{3}H	Anion/ cation	Remarks
89	10.08.	SVY 97-20	SP	X	X	X	-	Snowfield
90	10.08.	SVY 97-21	SP	X	X	X	-	Snowfield
91	10.08.	SVY 97-22	SP	X	X	X	-	Snowfield
92	10.08.	SVY 97-23	SP	X	X	X	-	Snowfield
93	10.08.	SVY 96-14	SW	X	X	X	-	Lake Dering Kuyel'
94	11.08.	KOL 95-1	RIW	X	X	X	-	Kolychev (SW-Bykovsky Peninsula)
95	11.08.	KOL 95-2-1	RIW	X	X	X	-	1,0 m,
96	11.08.	KOL 95-2-2	RIW	X	X	X	-	0,8 m,
97	11.08.	KOL 95-2-3	RIW	X	X	X	-	0,6 m,
98	14.08.	TIK 99-5	RW	X	X	X	-	
99	10.08.	SVY-1-4	SP		X	X	-	Snowfield, Sevastyan River, CAF
100	10.08.	SVY-1-5	SP		X	X	-	CAF
101	10.08.	SVY-1-6	SP		X	X	-	CAF
368	04.09.	MKH-02-1.0	IW	X	X	-	X	FROZEN
369	04.09.	MKH-02-1.1	IW	X	X	-	X	FROZEN
370	04.09.	MKH-02-1.2	IW	X	X	-	X	FROZEN
371	04.09.	MKH-02-1.3	IW	X	X	-	X	FROZEN
372	04.09.	MKH-02-1.4	IW	X	X	-	X	FROZEN
373	04.09.	MKH-02-1.5	IW	X	X	-	X	FROZEN
374	04.09.	MKH-02-1.6	IW	X	X	-	X	FROZEN
375	04.09.	MKH-02-1.7	IW	X	X	-	X	FROZEN
376	04.09.	MKH-02-1.8	IW	X	X	-	X	FROZEN
377	04.09.	MKH-02-1.9	IW	X	X	-	X	FROZEN
378	04.09.	MKH-02-1.10	IW	X	X	-	X	FROZEN
379	04.09.	MKH-02-1.11	IW	X	X	-	X	FROZEN
380	04.09.	MKH-02-1.12	IW	X	X	-	X	FROZEN
381	04.09.	MKH-02-1.13	IW	X	X	-	X	FROZEN
382	04.09.	MKH-02-1.14	IW	X	X	-	X	FROZEN
383	04.09.	MKH-02-1.15	IW	X	X	-	X	FROZEN
384	04.09.	MKH-02-1.16	IW	X	X	-	X	FROZEN
385	04.09.	MKH-02-1.17	IW	X	X	-	X	FROZEN
386	04.09.	MKH-02-1.18	IW	X	X	-	X	FROZEN
387	04.09.	MKH-02-1.19	IW	X	X	-	X	FROZEN
388	04.09.	MKH-02-1.20	IW	X	X	-	X	FROZEN
389	04.09.	MKH-02-1.21	IW	X	X	-	X	FROZEN
390	04.09.	MKH-02-1.22	IW	X	X	-	X	FROZEN
391	04.09.	MKH-02-1.23	IW	X	X	-	X	FROZEN
392	04.09.	MKH-02-1.24	IW	X	X	-	X	FROZEN
393	04.09.	MKH-02-1.25	IW	X	X	-	X	FROZEN
394	04.09.	MKH-02-1.26	IW	X	X	-	X	FROZEN
395	04.09.	MKH-02-1.27	IW	X	X	-	X	FROZEN
396	04.09.	MKH-02-1.28	IW	X	X	-	X	FROZEN
397	04.09.	MKH-02-1.29	IW	X	X	-	X	FROZEN
398	04.09.	MKH-02-1.30	IW	X	X	-	X	FROZEN
399	04.09.	MKH-02-1.31	IW	X	X	-	X	FROZEN
400	04.09.	MKH-02-1.32	IW	X	X	-	X	FROZEN
401	04.09.	MKH-02-1.33	IW	X	X	-	X	FROZEN
402	04.09.	MKH-02-1.34	IW	X	X	-	X	FROZEN
403	04.09.	MKH-02-1.35	IW	X	X	-	X	FROZEN
404	04.09.	MKH-02-1.36	IW	X	X	-	X	FROZEN
405	04.09.	MKH-02-1.37	IW	X	X	-	X	FROZEN
406	04.09.	MKH-02-1.38	IW	X	X	-	X	FROZEN
407	04.09.	MKH-02-1.39	IW	X	X	-	X	FROZEN
408	04.09.	MKH-02-1.40	IW	X	X	-	X	FROZEN

Appendix 4-2. continuation.

No.	Date	Sample	Type	^{18}O	^{2}H	^{3}H	Anion/ cation	Remarks
409	04.09.	MKH-02-1.41	IW	X	X	-	X	FROZEN
410	04.09.	MKH-02-1.42	IW	X	X	-	X	FROZEN
411	05.09.	OPE-1	SW	X	X	-	X	FROZEN
412	05.09.	OPE-2	SW	X	X	-	X	FROZEN
413	05.09.	OPE-3	SW	X	X	-	X	FROZEN
414	07.09.	TIK-SP-1	SP	X	X	X	-	

Abbreviations : SP = Snow patch; RW = rain water; IW = ice wedge ice; RIW = recent ice wedge ice ; SW = surface water; GW = ground water; TI = texture ice; CAF = cellulose acetat filter

4.8 References

Drachev, S.S., Savostin, L.A., Groshev, V.G., Bruni I.E. (1998): Structure and geology of the continental shelf of the Laptev Sea, Eastern Russian Arctic,. Tectonophysics 298: 357-393.

Franke, D., Krüger, F. & Klinge, K. (2000): Tectonics of the Laptev Sea – Moma 'rift' region: investigation with seismologic broadband data.- J. of Seismology, 4: 99-116.

Galabala (1980): New data on the structure of Lena Delta.- In: Chetvertichny period Severo-Vostoka Asii (Quaternary period of Northeast Asia).- Magadan:SVKNII DVO AN SSS%: 152-171 (In Russian).

Galabala, R.O. (1997): Pereletki and the initiation of glaciation in Siberia.- Quat. Int. 41/42: 27-32.

Grigoriev, M (1993): Cryomorphogenesis in the Lena Delta.- Permafrost Institute Press, Yakutsk, pp. 176 (In Russian).

Grosswald, M.G., Spektor, V.B. (1993): The glacial relief of the Tiksi region (west shore of Buor-Khaya inlet, Northern Yakutia.- Polar Geography and Geology, 17/2: 154-166.

Imaev, V.S., Imaeva, L.P. & Koz'min, B.M. (2000): Seismotektonika Yakutii,- GEOS, Moscow, pp. 226.

Katasonova, E.G. (1963): The role of thermokarst for the development of delly; In: Uslowya i osowennosti raswitya merslykh toltsch w Sibiri i na Sewero-Wostokye; Moscow; 91-100; (In Russian).

Kunitsky, V., Schirrmeister, L., Grosse, G., Kienast, F. (2002): Snow patches in nival landscapes and their role for the Ice Complex formation in the Laptev Sea coastal lowlands, Polarforschung, 70: 53-67.

Kunitsky, V.V. (1987): Role of glaciers and snow patches for cryolithogenic formations in the lower Lena area.- Theses of dissertation, cand. geograph science, Yakutsk, 21 pp. (In Russian).

Kunitsky, V.V. (1989): Cryolithology of the lower Lena.- Permafrost Institute Yakutsk, 164 pp. (In Russian).

Parfenov, L.M. (ed.) (2001): Tektonika, Geoidynamika i Metallogeniya territorii Respublik Sakha (Yakutiya) (Tectonik, Geodynamics and metallogeny of Sakha Republic, Yakutia).- Russian Academy of Science "Nauk/Interperiotika",pp 571 (In Russian).

Schirrmeister, L., Siegert, C., Kuznetsova, T., Kuzmina, S., Andreev, A.A., Kienast, F., Meyer, H., Bobrov, A.A. (2002): Paleoenvironmental and paleoclimatic records from permafrost deposits in the Arctic region of Northern Siberia, Quaternary International 89: 97-118.

Siegert, C., Schirrmeister, L., Kunitsky, V.V., Sher, A.,Tumskoy, V., Meyer, H. (1999): Paleoclimate signals of ice-rich permafrost; In: Russian-German Cooperation System Lapev Sea 2000: The Lena Delta 1998 Expedition (ed: Rachold, V. & Grigoryev, M.N.); Reports on Polar Research, 315: 145-190.

Slagoda, E.A. (1993): Genesis and microstructure of cryolithogenic deposits at the Bykovsky Peninsula and the Muostakh Island. Thesis, RAS Siberian section, Permafrost Institute, Yakutsk, pp 218 (In Russian).